



UNIVERSITÀ
DEGLI STUDI
FIRENZE

FLORE

Repository istituzionale dell'Università degli Studi di Firenze

Nanoparticles and organized lipid assemblies: from interaction to design of hybrid soft devices

Questa è la Versione finale referata (Post print/Accepted manuscript) della seguente pubblicazione:

Original Citation:

Nanoparticles and organized lipid assemblies: from interaction to design of hybrid soft devices / Marco Mendoza, Lucrezia Caselli, Annalisa Salvatore, Costanza Montis, Debora Berti. - In: SOFT MATTER. - ISSN 1744-6848. - STAMPA. - 15:(2019), pp. 8951-8970. [10.1039/C9SM01601E]

Availability:

The webpage <https://hdl.handle.net/2158/1175074> of the repository was last updated on 2022-06-01T15:59:52Z

Published version:

DOI: 10.1039/C9SM01601E

Terms of use:

Open Access

La pubblicazione è resa disponibile sotto le norme e i termini della licenza di deposito, secondo quanto stabilito dalla Policy per l'accesso aperto dell'Università degli Studi di Firenze (<https://www.sba.unifi.it/upload/policy-oa-2016-1.pdf>)

Publisher copyright claim:

La data sopra indicata si riferisce all'ultimo aggiornamento della scheda del Repository FloRe - The above-mentioned date refers to the last update of the record in the Institutional Repository FloRe

(Article begins on next page)

REVIEW

Nanoparticles and organized lipid assemblies: from interaction to design of hybrid soft devices

Marco Mendoza, Lucrezia Caselli, Annalisa Salvatore, Costanza Montis* and Debora Berti*

Received 00th January 20xx,
Accepted 00th January 20xx

DOI: 10.1039/x0xx00000x

This contribution reviews the state of art on hybrid soft matter assemblies composed of inorganic nanoparticles (NP) and lamellar or non-lamellar lipid bilayers. After a short outline of the relevant energetic contributions, we address the interaction of NPs with synthetic lamellar bilayers, meant as cell membrane mimics. We then review the design of hybrid nanostructured materials composed of lipid bilayers and some classes of inorganic NPs, with particular emphasis on the effects on the amphiphilic phase diagram and on the additional properties contributed by the NPs. Then, we present the latest developments on the use of lipid bilayers as coating agents for inorganic NPs. Finally, we remark the main achievements of the last years and our vision for the development of the field.

1. Introduction

Lipid bilayers are ubiquitous structural motifs in natural and synthetic soft matter assemblies. Their interaction with nanostructured matter, and in particular with nanoparticles (NPs), is therefore of interest both for natural and engineered systems. In addition, the shared length and energy scales, combined with the peculiar properties of inorganic matter at the nanoscale, can be harnessed to use NPs to probe selected physical properties of membranes or to modify the amphiphilic phase diagram under external *stimuli*. In this contribution we will review the state of the art concerning research on hybrid soft matter assemblies composed of inorganic NPs and synthetic lipid bilayers, either in lamellar or non-lamellar arrangement. This topic is currently a very active area of research, with implications ranging from the design of smart nanostructured hybrid devices, where nanoparticles are included or functionalized with lipid bilayers, to the quest for mechanistic understanding of events taking place at the nano-bio-interface, relevant for nanomedicine and toxicity of nanomaterials. This review will focus on some selected classes of inorganic nanomaterials, namely metals (Au and Ag), metal oxides (like iron and zinc oxide) and silica NPs. The interaction of several other kinds of nanomaterials with lipid bilayers has been described in the literature and we refer the readers to some excellent recent reports on these topics^{1–8}.

In this contribution, particular attention will be devoted to non-covalent interactions that take place when NPs and lipid bilayers are put into contact. Understanding the nature and the key determinants of these interactions is instrumental both for fundamental and applied soft matter research.

This review is organized as follows: a short theoretical section will introduce the main energetic contributions at stake when NPs interact with lipid bilayers (section 2). Then, we will provide an overview of the most relevant studies which have recently addressed the interaction of NPs with synthetic phospholipid bilayers, meant as simplified and highly controllable mimics of cell membranes (section 3). In this section, we will emphasize some examples where the investigation on model systems contributed disclosing non-covalent interactions at play in living systems. Then, we will review (section 4) the design of hybrid nanostructured materials composed of lipid bilayers and inorganic nanoparticles, with particular emphasis on the effects on the amphiphilic phase diagram and on the additional properties contributed by the NPs. Then, we will present the latest developments on the use of lipid bilayers as coating agents for inorganic NPs (section 5), whose aim is the improvement of dispersibility, biocompatibility and pharmacokinetic properties. Finally, a conclusive paragraph will remark the main achievements of the last years and our vision for the development of the field.

Department of Chemistry “Ugo Schiff”, University of Florence, and CSGI (Italian Center for Colloid and Surface Science, Via della Lastruccia 3, Sesto Fiorentino, 50019 Firenze.

Electronic Supplementary Information (ESI) available: [details of any supplementary information available should be included here]. See DOI: 10.1039/x0xx00000x

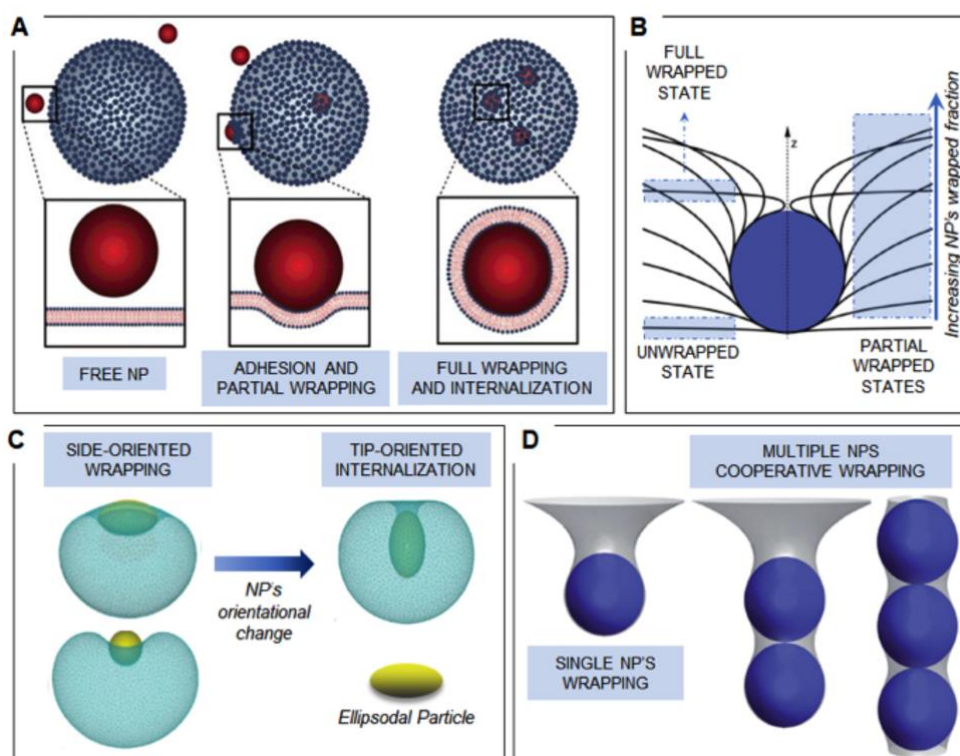


Figure 1 Theory of NPs-lipid membranes interactions. *Panel A* Illustration of the three possible configurations for a NP interacting with a lipid membrane: from left to right, (i) NP free in the environment (repulsive contribution to the NP-bilayer total interaction overcoming the attractive one), (ii) NP's adhesion to the membrane, causing NP's partial wrapping and (iii) NP's full engulfment (strong attractive NP-bilayer forces). Readapted from open access reference¹³. *Panel B* Illustrative picture representing unwrapped, fully wrapped and different wrapping degree-intermediate configurations for a NP interacting with a fluid interface. Reproduced from Ref.¹⁰¹ with permission from The Royal Society of Chemistry. *Panel C* Ellipsoidal NP's reorganization from a side-oriented configuration, adopted during the wrapping process, to a tip-oriented configuration, minimizing the energy required for full NP's engulfment and internalization. Reproduced from Ref.¹⁶ with permission from The Royal Society of Chemistry. *Panel D* Illustrative picture of (from left to right) a single NP wrapped by a fluid interface, two and three NPs wrapped in a membrane tube. Reproduced from Ref.¹⁰¹ with permission from The Royal Society of Chemistry.

2. Interaction of Nanoparticles with Lipid Membranes: the role of non-covalent forces

In this section we will consider the events following the exposure of a free-standing synthetic lipid bilayer to NPs, outlining the different contributions to the total interaction energy.

2.1 Theoretical description of NPs-lipid membrane interaction

The interaction between a NP and a lipid bilayer might lead to NP's adhesion on the bilayer, which can be followed by partial or total engulfment by the membrane. In a well-defined medium and at a given temperature, the NP docking to lipid membranes is thermodynamically favoured if the adhesion energy $E_{adh} < 0$, i.e., if the attractive terms overcome the repulsive ones. Considering a prototypical model of bioinorganic interface, with a spherical NP of radius R interacting with a liposomal membrane with curvature $1/R_0$, the energetic balance between repulsive and attractive forces can be approximately described by a classical DLVO (Derjaguin-Landau-Verwey-Overbeek) formalism, as in eq. (1), including only the electrical double layer (E^{EL}) and the London-Van der Waals (E^{LW}) contributions to the total energy of adhesion:

$$E_{adh} = E^{EL} + E^{LW} \quad (1)$$

Where the terms E^{EL} , derived as a combination between the linear Debye-Huckel and the Derjaguin approximations and valid for surface potentials < 25 mV, and E^{LW} are described in eq. (2) and (3), respectively:

$$E^{EL} = \frac{\varepsilon R_1 R_2 (\psi_1^2 + \psi_2^2)}{4(R_1 + R_2)} \left[\frac{2\psi_1 \psi_2}{(\psi_1^2 + \psi_2^2)} \ln \left(\frac{1 + e^{-kd}}{1 - e^{-kd}} \right) + \ln(1 - e^{-2kd}) \right] \quad (2)$$

$$E^{LW} = -A \frac{R_1 R_2}{6(R_1 + R_2)} \left(\frac{1}{d} - \frac{1}{(d+h)} \right) - \frac{A}{6} \ln \left(\frac{d}{d+h} \right) \quad (3)$$

Where ψ_1^2 and ψ_2^2 are the surface potentials of the NP and the membrane, d the NP-membrane distance, k the Debye length, h the membrane's thickness, and A is the Hamaker constant. Although the DLVO theory generally succeeds in predicting the colloidal stability of hard colloids (e.g. inorganic NPs) suspended in a liquid medium, it often fails in describing the interaction of NPs with free-standing bilayers; a more comprehensive description for E_{adh} includes additional repulsive hydration forces establishing at short NPs-membrane distances, as well as hydrophobic NP-lipid chain attraction (the interested reader is referred to a recent report for the analytical expression of these two supplementary energetic contributions⁹).

Once the NP is adsorbed onto the lipid surface (i.e. $E_{adh} < 0$), the elastic properties of the membrane comes into play, and their balance with the adhesion forces determines the degree of

membrane deformation and NP's wrapping. Specifically, the energetic gain due to the adhesion forces is maximized by increasing the contact area between the NP and the lipid membrane, according to equation (4)¹⁰:

$$E_{adh} = -w \int_0^{S_{ad}} dS \quad (4)$$

with w adhesion energy per unit area and S_{ad} the contact area between the membrane and the NP. On the other side, the NP's wrapping is associated with a free energy cost of imposing membrane deformation (E_{el}), which is expressed through the Cahn-Helfrich-Evans formalism¹⁰:

$$E_{el} = \int_0^S dS [\gamma + 2k_B(H - c_0)^2 + \bar{k}K] \quad (5)$$

with S the entire interfacial area.

As we can see from eq. (5), the deformation penalty depends both on the membrane's topology, through the mean H and Gaussian K curvatures, and on the interface's mechanical and elastic properties, expressed by the surface tension γ , bending rigidity k_B , spontaneous curvature c_0 and Gaussian saddle splay modulus \bar{k} . It is the fine interplay between E_{adh} and E_{el} that ultimately defines the NP-membrane arrangement which minimizes the system's energy, ranging from completely unwrapped NPs (e.g. for small nanoparticles and/or weakly interacting with the lipid phase), to larger and/or strongly adhered nano-objects, eventually fully engulfed by the lipid membrane (See Figure 1A).

Based on the above treatment, we will now discuss the several NPs- and membrane-related factors implicated in this interaction, with particular attention on size, shape, surface coating of NPs and NP-NP correlations; on the "membrane" side, we will take into account some selected physicochemical properties and the zero or non-zero curvature.

Depending on their size, the adhesion of NPs on a target planar membrane can result in different effects: small NPs can either remain embedded in the lipid membrane or directly diffuse through it; relatively larger particles (>10 nm) can be wrapped by the membrane¹¹. This process is finely controlled by the energetic balance between the adhesion forces (eq. (4)) and the membrane's elastic deformation penalty (eq. (5)) leading to an optimal size for wrapping, as first observed by Roiter et al.¹². In particular, two characteristic NPs' limiting radii for a successful engulfment by lipid membranes can be theoretically predicted¹⁰:

$$R_{kw} = \sqrt{\frac{2k_b}{E_{adh}}} \quad (6)$$

$$R_{ky} = \sqrt{\frac{2k_b}{E_{adh} - \gamma}} \quad (7)$$

Within the bending-dominated regime (i.e. for relatively small membrane's deformation), the membrane tension can be neglected, and the wrapping process is mainly controlled by the competition between membrane's bending and NP's adhesion

strength, defining a critical radius R_{kw} . NPs with $R < R_{kw}$ remain unwrapped, while larger NPs ($R > R_{kw}$) are fully engulfed inside the lipid scaffold. For larger membrane's deformation (e.g. induced by micron-sized particles), a characteristic length scale $\lambda = (2k_b/\gamma)^{1/2}$, which depends solely on membrane's properties, marks the crossover from the bending-dominated to the stretching-dominated regime^{9,13} (Figure 1 B), where the γ -dependent wrapping extent gradually increases with NP's size. The full engulfment is reached for a second crossover NP's radius R_{ky} (eq. (7)), representing a larger NP's limiting size, which is required for the internalization in the case of finite tension-membranes.

2.2 Key NPs features in the interaction with lipid membranes

Concerning NPs shape, the increase of the surface area/volume ratio from spherical to asymmetrical NPs (e.g. nanorods, nanoprisms and nanocubes), maximizes the surface available for absorption onto lipid membranes (eq. (4)), enhancing their reactivity¹⁴; on the other side, the local particle's surface curvature is predicted to increase the energy barrier associated to membrane's deformation, stabilizing partial-wrapping states also for tensionless membranes^{9,10}. Moreover, the interaction of asymmetric NPs with target lipid membranes can lead to preferential wrapping orientations, to minimize the energy cost for wrapping^{15,16} (See Figure 1C). Eventually, the asymmetric shape of NPs can drive peculiar self-assembly phenomena at the nano-bio interface, some examples of which are given in Section 3.

The NPs surface functionalization represents another important factor affecting the interaction with membranes; in particular, NPs surface charge has a major impact on adhesion both onto charged and zwitterionic interfaces, setting the sign and magnitude of the electrostatic long-range contribution of (eq.1)^{3,17–21}. Furthermore, the adhesion of charged NPs to a target membrane is also associated to an entropic gain, deriving from the release of small counterions from the NP surface²² (See Figure 1D). On the other side, the presence of polymeric steric stabilizers on the NPs surface, like for PEGylated particles, often decreases the adhesion energy; this effect can be understood considering the mobility loss experienced by the polymer chains approaching the lipid surface, which entails a considerable entropic penalty for membrane adhesion. Moreover, NPs' surface functionalization determines their polarity, which is key in controlling their spontaneous localization when challenging a free-standing lipid membrane: generally, hydrophilic nanomaterials with size larger than 10 nm reside at the membrane surface, with the possibility to be partially or fully wrapped by the membrane. Conversely, depending on their hydrophobicity²³, small particles can either spontaneously cross^{24,25} or be entrapped²⁴ within the lipid membrane, provoking an alteration of the bilayer's frustration packing energy^{26–31}.

Eventually, interparticle forces between different membrane-bound NPs may originate cooperative phenomena, ultimately leading to the simultaneous wrapping and engulfment of

multiple NPs (see Figure 1D), which will be discussed in detail in section 3.

2.3 Key membrane features in the interaction with NPs

Membrane-related characteristics have a crucial role in the interaction with NPs. In particular, the composition of lipid bilayers determines specific physico-chemical, viscoelastic and thermodynamic properties of relevance in the interaction with NPs. Membrane's surface potential, determined by the percentage of non-ionic, anionic and cationic lipids, strongly affects the electrostatic contribution to NPs adhesion (eq. 1) while the presence of specific components (e.g. cholesterol) and their relative abundance, give rise to characteristic behaviours, which will be extensively discussed in section 3.

Equally important, the molecular geometry of the membrane's components determines the equilibrium arrangement of lipids within the bilayer. The molecular packing represents the main factor affecting both the physical state and the overall topological curvature of membranes, which are two prominent determinants in the interactions with nanomaterials.

In particular, the interactions at the nano-lipid interface is extremely affected by the gel-liquid crystalline phase behaviour of lipid membranes: by increasing temperature, lipid bilayers undergo a main phase transition from the so-called "gel state" (L_β), where hydrocarbon chains are tightly packed and almost locked in place, to a "fluid state" (L_α), where lipids freely diffuse within the 2D membrane's plane. The "melting transition temperature" (T_m) is specific for a given lipid composition and determines the elastic response of membranes at a given temperature. In particular, gel phase bilayers show a reduced reactivity with nanomaterials, mostly due to the high value of their bending rigidity (k_B) with respect to the fluid phase, which strongly hampers the membrane's bending and wrapping around NPs (see eq. (5-7)). On the other side, the interaction with NPs, which can proceed through polar headgroups (hydrophilic NPs) or hydrophobic chains (hydrophobic NPs) might affect the lipid molecular packing, leading to micro and macroscopic modifications in the membrane structure and thermotropic behaviour (specific examples will be provided in the following paragraphs).

As predicted from eq.5, the membrane's topology plays a crucial role in its elastic response to NP's induced deformations. Although lipid membranes are generally visualized as flat bilayers (H and G in eq. (5) equal to zero), both biomembranes and synthetic lipid assemblies may fold into more organized non-lamellar bilayered structures³². The interaction of nanomaterials with such non-lamellar structures may have a noteworthy relevance both for biomimetic and technological applications^{33,34}, (as discussed in details in the following paragraphs) while it remains, to date, a highly unexplored research area.

Differently from planar membranes, curved membranes are defined by positive (direct phases) or negative (inverse phases) mean curvature (H) and non-zero Gaussian curvature (K)³⁵ in

each point of their surface, with H and G described by eq. 8 and 9, respectively:

$$H = \frac{1}{2}(c_1 + c_2) \quad (8)$$

$$K = c_1 c_2 \quad (9)$$

with c_1 and c_2 minimum and maximum values of curvature at a specific point of membrane surface.

The non-zero values of H and K lead, as predicted from eq. (5), to a modification of their Helfrich energy and elastic response towards externally induced deformations (e.g. NPs' wrapping) with respect to the case of lamellar membranes. Moreover, different topologies are associated with a frustration packing free energy (E_P), which varies according to eq. (10)³⁶:

$$E_P = k(l - l_r)^2 \quad (10)$$

with k stretching rigidity of lipid chains, l and l_r hydrophobic chain extension in the stretched and relaxed state, respectively. Phase transitions between different geometries, including changes in both elastic and frustration packing energies, have high biological relevance, sharing similar energy barriers and molecular re-arrangements with membrane fusion processes³⁷. Several recent studies, which will be addressed in section 4, demonstrated that both hydrophilic and hydrophobic NPs can promote phase transitions between model mesophases with different geometry^{26,27,34,37-41}, lowering the energy barrier required to switch from low to high curvature phases. One of the first attempts to elucidate this effect is represented by recent works^{26,42}, where the transition temperature from cubic to hexagonal phases in monoolein liquid crystals is demonstrated to be finely controlled by inclusion of hydrophobic iron oxide NPs (see section 4). This behaviour was explained by combining the Helfrich theory in eq. (5) with geometrical considerations: NPs increase the frustration packing energy of the cubic phase (eq. (10)), while they have a milder effect on the hexagonal arrangement, by inserting into its hydrophobic voids (See Figure 2).

In the framework of this theoretical description, in recent years the interaction of NPs with lipid membranes has been

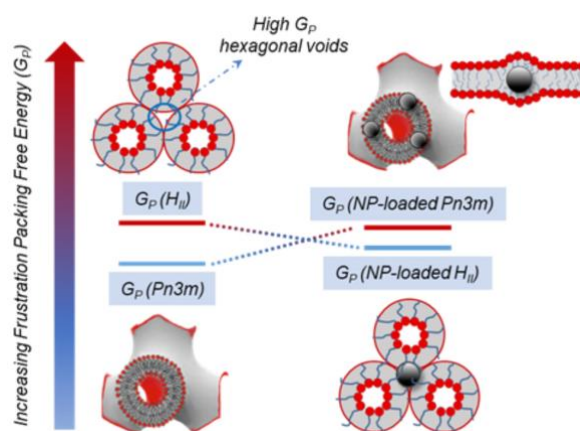


Figure 2 Effects of NPs on lipid mesophases architectures. Illustrative scheme of the NP-induced modification of the Frustration Packing Energy of both cubic and hexagonal mesophases.

explored with different approaches and for different purposes from fundamental studies employing lipid bilayers biomimetic platforms of tuneable physicochemical feature investigating the interaction with prototypical nanoparticles aimed at a better understanding of the efficiency and possible adverse effects of nanomaterials designed for biomedical applications, to applicative studies, where the interaction of NPs and lipid membranes is exploited for analytical purposes from the engineering of lipid assemblies with NPs inclusion, in order to form smart hybrid materials for applications in materials science, to the functionalization of NPs with a lipid coating, to improve their biocompatibility and pharmacokinetic properties.

In section 3 we will review the interaction of NPs with synthetic lipid bilayers, taken as simplified models of real plasma membranes: in line with section 2, we will consider the main physicochemical factors, either related to NPs or to the lipid membrane, affecting the interaction under simplified conditions. We will provide relevant examples from the recent literature, highlighting the connections, whenever they are relevant, between the findings on cell models and the *in vitro*/*in vivo* observations.

3. NPs/biomembrane Interactions: from biophysical studies of nano-bio interfaces to applications

One of the main issues limiting the development of nanomedicine and the translation of engineered nanomaterials into medical practice, is the poor understanding of their fate in biological fluids, and their short-term and long-term possible adverse cytotoxic effects^{37,43–49}. Recent reports have also highlighted how nanodevices designed for nanomedicine applications, whose functionality/efficiency has been proved at the lab-scale, completely fail reaching their biological targets once in a living organism⁵⁰. As a matter of fact, to date, nanotherapeutics available on the market are mainly limited to polymeric- and liposomal-based formulations^{51,52}, while, apart from some iron oxide NPs-based formulations, inorganic and metallic particles are at research stage or in clinical trials.

With the ultimate aim to fill the gap between the design/synthesis/development of nanomaterials for nanomedicine and their end use application, it is necessary to improve our fundamental knowledge on the interaction of nanomaterials with biologically relevant interfaces, particularly cell membranes.

Plasma membrane, primarily composed by a mixed phospholipid bilayer with embedded proteins, protects the interior and ensures its communication with the external environment. The mechanisms of cell signalling processes are extremely complex and length scale-dependent, with small molecules spontaneously crossing the lipid barrier and large and/or polar molecules harnessing protein-mediated transportations across the membrane¹³. The nanoscale, shared by engineered particles and biologically relevant

macromolecules (i.e., DNA, viruses, surface proteins), is mostly associated with endocytic pathways, where the internalisation of nano-objects is generally controlled by the membrane through specific receptor-protein binding for the case of biological species^{54,55}. However, it has been demonstrated that synthetic NPs can be wrapped and internalized by both model and real cell membranes in the absence of any receptor-mediated interaction^{43,55,56}, under exclusive control of non-specific interactions taking place at the nano-bio interface, and membrane's elasticity.

In this context, synthetic lipid membranes (together with more complex systems, as organ-on-a-chip and 3D cells arrays, mimicking an entire tissue⁵⁷), are interesting biomimetic systems, which, by mimicking the main structural unit of plasma membranes, allow investigating phenomena at the nano-bio interface in simplified and highly controlled conditions^{44,45,58}.

In recent years, both experimental and theoretical studies have addressed the interaction of NPs with synthetic lipid membranes, aimed at establishing clear connections between the results in simplified model systems and what observed in real cells, in order to enabling predictive strategies for the design of evermore efficient and non-toxic nanomaterials for nanomedicine.

In the following sections recent relevant studies on NPs-synthetic lipid membranes interactions, together with their implications for the understanding of real nano-bio interfaces, will be revised, particularly focusing on: the effect of NPs coating (surface charge, exchangeability of the ligand, steric hindrance of the coating, impact of the protein corona) (3.1); the effect of NPs size and shape (with particular interest on the relevance of NPs clusterization in cell uptake) (3.2); the effect of NPs adhesion on the composition, integrity and viscoelastic properties of the target membrane (3.3). In addition, the interaction of inorganic NPs and lipid membranes has been exploited for analytical purposes, in order to label/signal/probe selected properties of cells or lipid assemblies in complex biological media, both exploiting specific and non-specific interactions of NPs with the target membranes. This latter research field will be reviewed in section 3.4.

3.1 Biophysics of nano-bio interfaces: NPs coating

3.1.1 NPs surface charge

The intrinsic characteristics of NPs (i.e., core composition, size, shape) often have a secondary impact on the interaction with a target lipid membrane, which is primarily mediated by the ligands coating the NP's surface: the surface characteristics of NPs determine polarity and interfacial properties, directly involved in the electrostatic and London-Van der Waals contributions to NPs' adhesion to a lipid interface (see paragraph 2.1 for the theoretical background). The interaction of NPs with target membranes is primarily affected by the charge of both components (see equation 2). In order to closely resemble real plasma membranes, most of the employed model bilayers in biomimetics are characterized by a zwitterionic or slightly anionic nature. Therefore, negatively charged NPs tend to be electrostatically repelled from the

membrane, undergoing to weaker interactions with respect to cationic ones: remarkably, this is also observed for real cell membranes, where the uptake is generally much lower for anionic NPs than for cationic ones^{59–61}. However, the situation of real cells is complicated by the presence of other interaction pathways of specific nature, representing an alternative with respect to non-specific forces. Several studies have highlighted that nonionic, anionic and cationic NPs of similar sizes undergo different internalization routes, from clathrin- or caveola-mediated endocytosis to non-endocytic pathways, like passive diffusion^{62,63}. Even if characterized by limited interaction capability, yet anionic NPs are attractive for biomedical applications, due to limited adverse cytotoxic effects. In addition, despite the dominantly repulsive electrostatic forces, several reports have shown successful internalization of anionic NPs, as silica or Gold NPs (AuNPs)^{63–65}. Conversely, cationic NPs have a strong tendency to interact with negatively charged

membranes: it has been shown that cationic NPs adhere and clusterize onto synthetic target membranes, extract lipids from the membrane, ultimately provoking localized membrane disruption or integrity loss^{22,66,67}. In line with this findings, they are often characterized by limited stability in biological media and, above all, relevant toxic effects on real cells^{13,68,69}. Recently, Lee et al.⁷⁰ hypothesized, by means of a systematic study using a charge library of modified AuNPs, that the magnitude of the positive charge is not the sole factor determining the extent of interaction with target membranes and, thereby cytotoxicity. They conclude that spatial proximity of positively charged functional groups within a hydrophobic moiety is a common characteristic of toxic gold colloids.

3.1.2 NPs coated with steric stabilizers

A common strategy to increase the colloidal stability of NPs in biological media consists in the passivation of NPs with bulky ligands, to endow them with steric stabilization. This kind of coating also improves the pharmacokinetic properties of NPs: For instance, it is well known that PEGylation prevents opsonisation, improving the circulation time of the nanomaterial. This stealth effect of PEG in preventing opsonisation depends on its steric hindrance: it has been shown that both NPs uptake and circulation time depend on the molecular weight of PEG coating the NPs⁷¹. Moreover, thanks to molecular dynamic simulations, Lin et al.⁷² elucidated the effect of both the grafting density and polymer's chain length on the shielding ability of PEG layers bounded to gold NPs of varying size. Similar examples of steric stabilization of NPs have recently been proposed by Jiang and co-workers, who have employed poly(zwitterionic)protein functionalization (for instance poly(carboxybetaine)) to improve pharmacokinetic properties of NPs^{73,74}, while other examples of polyzwitterionic coatings are poly(acrylic acid) derivatives, poly(maleic anhydride-alt-1-alkene) derivatives or poly(sulfobetaine) derivatives, which offer several advantages over PEGylation (see as a reference the Review from Garcia et al.⁷³).

PEGylation or steric stabilization affects the interaction of NPs with synthetic target membranes, with possible implications also at the real membranes' level. Indeed, the use of steric stabilizers, like PEG, is theoretically predicted to decrease the adhesion of NPs to lipid membranes, due to the high entropic loss associated to the adsorption process (see paragraph 2).

Through large scale molecular dynamic simulations, In a recent study⁷⁵, Gal and coworkers extensively characterized the interaction of PEGylated SPIONs of different size with both synthetic membranes of different composition and real cancer and kidney cells. In the frame of classic DLVO theory (paragraph 2), they presented a direct comparison of NP-synthetic and real membrane interactions, linking weak NP adsorption to anionic lipid membranes, due to NP-bilayer electrostatic interactions, with eukaryote cell uptake, without membrane penetration. Moreover, they showed that the NP-membrane electrostatic

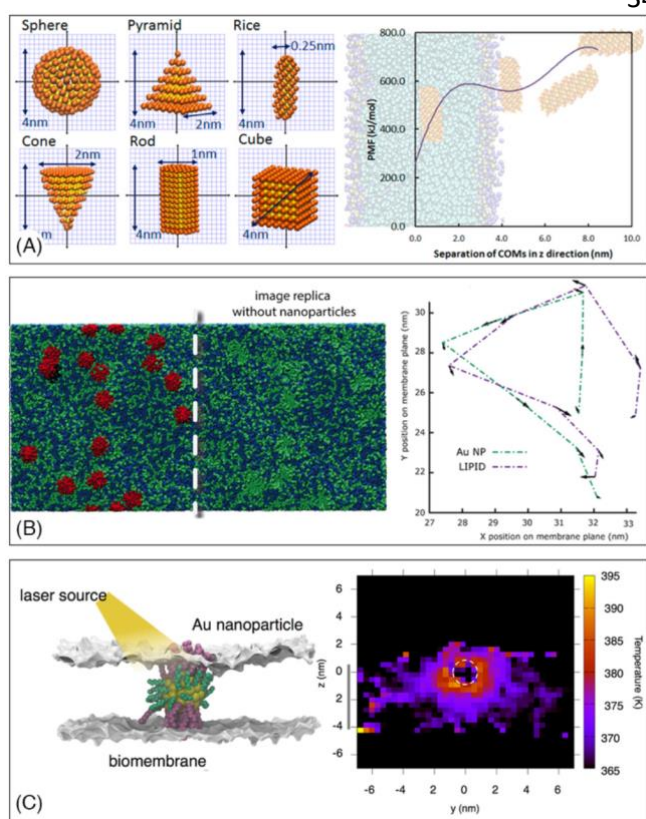


Figure 3 Theoretical studies on nano-bio interfaces. Panel (A) Molecular dynamics study to compute translocation rate constants of NPs of different shapes through lipid membranes; (left) coarse-grained gold nanoparticles setup; (right) analysis of rice NP translocation: potential of mean force, PMF (kJ/mol) profile as a function of distance of the NP from the lipid bilayer. Adapted with permission from¹⁰⁴. Copyright (2012) American Chemical Society. Panel (B) Lipid membrane modifications upon interaction with cationic gold NPs: (left) Lateral phase separation of 1:1 anionic (green) and zwitterionic (blue) lipids in the presence of gold NPs (red); (right) trajectories of NP (green) and anionic lipid (blue) highlighting the slowed diffusion of anionic lipids upon interaction with NPs. Adapted with permission from²². Copyright (2019) American Chemical Society. Panel (C) Nonequilibrium molecular dynamics simulations to investigate photoporation of lipid membranes through the irradiation of AuNPs: the NPs, stably bound to cell membranes, convert the radiation into heat; a quantitative prediction of the temperature gradient around the NP upon irradiation is evaluated. Adapted with permission from¹⁹⁷ Copyright (2017) American Chemical Society.

attraction is suppressed by increasing PEG molecular weight and NP size, which they correlated with low cell uptake and cytotoxicity in two cell lines.

A common strategy to circumvent the poor ability of sterically stabilized NPs to interact with cells *via* non-specific interactions, limiting their cell uptake and therapeutic/diagnostic efficiency is to exploit exploiting NP-membrane specific interactions which are available for the case of real plasma membranes. Endowing NPs surface with targeting moieties, might result in promoting the effective docking of NPs on cell membranes and improving the successful achievement of their biological target. For instance, in a proof-of-concept study it was shown that adding biotin or streptavidin moieties allows specific binding of polymer-coated NPs to beads carrying the complementary unit⁷⁶; Kaaki et al.⁷⁷ highlighted the efficient targeting of human breast carcinoma cells by folic acid-conjugated iron oxide NPs with a PEG coating; however, partially contradictory results were obtained by Kraiss et al. on similar system, where folate-dependent targeting was highlighted⁷⁸.

3.1.3 NPs coating with exchangeable ligands

The binding mode and strength between the NPs and the coating agent determine both single NP-membrane interactions and collective NP-NP interactions at the nano-bio interface. Physisorbed ligands, which can be easily displaced from the NP's surface through ligand-exchange, are associated to enhanced reactivity of NPs, which can be considered as "naked". Recently, hydrophobic physisorbed ligands, i.e. oleic acid/oleylamine coatings on iron oxide NPs, have been associated to small NPs' pearl-necklace aggregation inside monoolein bilayers²⁶. Moreover it has been shown that hydrophilic weakly adsorbed ligands on the surface of AuNPs can promote peculiar aggregation phenomena occurring on the lipid membrane^{18,19}, which are particularly significative also for the case of repulsive NPs/membrane electrostatic interactions (e.g. between negatively charged gold NPs and slightly anionic synthetic free-standing bilayers). Moreover, weakly bound physisorbed ligand onto the NPs surface can be easily replaced with other molecules establishing covalent or stronger non-specific interaction with the bare NPs surface: remarkably, it has been recently demonstrated by Wang et al.⁷⁹, that weak ligands as citrate and short DNA fragments onto the gold surface, can be effectively replaced with lipid components of cell membranes, resulting in unique interfacial phenomena. Indeed when ligand exchange processes occur at the interface, NPs might aggregate into ordered monolayers on the lipid membrane, which might affect membrane integrity and internalization efficiency and pathway.

3.1.4 Protein corona coating of NPs

An interesting aspect is the functionalization of NPs surface with the so-called protein corona^{14,55,80,81}. From the pioneer studies of K. Dawson^{82–84} and coauthors, it has been progressively established that NPs in biological fluids spontaneously covered by a self-assembled layer of proteins, an inner non-exchangeable layer and an external exchangeable

one), which determines a "biological identity" of the NPs and, ultimately, their ability to interact with cells^{44,80,85,86}. The composition of the protein corona depends on the nature of NPs core, on their shape and on their surface coating. In particular, the surface charge of NPs also affects the adhesion of biomolecules present in biological media, modifying the protein corona, in terms of composition and orientation^{62,87,88}. It has also been highlighted that during NPs internalization, the tendency of corona proteins is, at least partially, to remain attached to NPs surface^{83,89,90}. Since proteins are generally characterized by significant steric hindrance and amphiphilic nature, they specifically mediate the interaction of the NPs with plasma membranes. In this context, it has been highlighted that slight physicochemical modifications of the proteins modify their binding and orientation on NPs, strongly affecting the biological uptake of NPs⁹¹. Recently, the controlled formation of the protein corona has been exploited both for application purposes (e.g., for applications in cancer vaccines⁹²) and also to control in a predictable way the protein-corona-mediated interaction of NPs with cell membranes. For instance, pre-incubation of NPs with serum has been exploited to prevent NPs aggregation in biological media, improve their cell uptake and decrease their cytotoxic effects⁶⁹. The comprehension, control and exploitation of protein corona formation is therefore a key milestone in determining and predicting NPs fate in living organisms.

3.2 Biophysics of nano-bio interfaces: NPs size and shape

As discussed in section 2, when a NP adheres to a planar lipid membrane, it locally imposes a curvature modification, which depends on the size of NPs and on the viscoelastic properties of the membrane (equation 5), which eventually controls the occurrence and extent of NPs wrapping by the membrane; therefore, NPs size also determines the response of the bilayer to its adhesion and, ultimately, the effects on the target membrane and the internalization pathway. NPs with size comparable or smaller than the lipid bilayer thickness can either be entrapped within the membrane³⁰ or translocate across the lipid bilayer by diffusing through^{25,93,94} or by opening pores in the membrane⁹⁵, which is normally associated to a high cytotoxicity *in vivo*^{56,96}. On the contrary, wrapping represents the dominant mechanism for larger particles (>10 nm) interacting with bilayers, which is associated to their entrance into cells in living organisms¹¹. Often, depending on NPs size, adhesion to a target membrane might result in the NPs clusterization: indeed, under specific conditions, membranes actively drive the self-assembly of adsorbed NPs, as a result of the tendency of the membrane to minimize the NP-induced deformation and its associated elastic cost (eq. 5)⁹⁷. As a result, small-sized NPs have been observed to preferentially interact with membranes as clusters^{67,98}, while fluid membranes have been theoretically predicted to mediate the asymmetric aggregation of spherical nanoparticles onto lipid surface⁹⁹. This aspect is particularly significant for medical application of nanomaterials, since NPs uptake in model and real membranes is often preceded by aggregation at the nano-bio interface¹¹. In addition, mathematical models and molecular dynamic simulations have revealed that membrane-induced interactions between bound particles can lead

to collective NPs wrapping and internalization: in particular, Zhang et al.¹⁰⁰ revealed that NPs translocation proceeds in a cooperative way with a key role played by NPs quantity, while Lipowsky et al.^{101,102} showed that spherical NPs can be cooperatively wrapped in tubular membrane invaginations.

While the effect of NP's size has been extensively investigated, much less is known on the impact of NP's geometry. Asymmetrically shaped NPs, like nanorods, nanodisks and nanostars, are particularly attractive materials, due to the peculiar properties (optical, magnetic, electronic and so on) arising from anisotropy.¹⁰³ Depending on their shape, anisotropic NPs can efficiently interact with a target membrane and translocate across it. MD studies on the interaction of NPs of different non-spherical shapes highlighted reorientation of NPs in proximity to the target membrane, to maximize the interaction, leading to strong shape and orientational dependence on the translocation¹⁰⁴ (See Figure 3A); in addition, it has to be considered that, from a theoretical standpoint, it is thermodynamically more favourable for a lipid membrane to wrap a spherocylinder than a sphere of the same radius.¹⁰⁵ Consistently with the theoretical predictions, non-spherical NPs, from nanostars to nanorods, are efficiently internalized by cells, in a shape and, for nanorods, aspect-ratio dependent manner.^{106,107} Experimental studies on biomimetic membranes have shown that the asymmetric shape of NPs can drive peculiar self-assembly phenomena at the nano-bio interface^{10,37}: as an example, we recently demonstrated

that gold nanorods (Au NRs) are wrapped by model and real cell membranes as end-to-end NPs' clusters⁶⁷, reducing the energy penalty required for the membrane to bend around highly curved edges. The induced tension due to the adhesion of asymmetric NPs determines effects of lipid extraction, observed both on model membranes and macrophage cells, eventually provoking extensive disruption of the membrane, related to a significant *in vitro* cytotoxicity⁶⁷.

3.3 Biophysics of nano-bio interfaces: Membrane composition

Cell membranes are characterized by a high degree of compositional heterogeneity, typically comprising of thousands of different lipids, carbohydrates and proteins¹⁰⁸, which is reproduced, at different complexity levels, by model membranes. The chemical composition of both synthetic and natural bilayers strongly affects their elasticity, physical state and structure, thereby determining their response towards external *stimuli*. A clear example is the recent work of Lunnø et al.¹⁰⁹, in which model bilayers with different compositional complexity levels correspond, as predicted by their proposed MD simulations, to diverse cellular uptake pathways of neutral 10-nm gold NPs. Going more into details, the presence of charges on the lipid membrane emphasizes the interaction with oppositely charged particles, as expected from eq. (2)⁹⁶ in

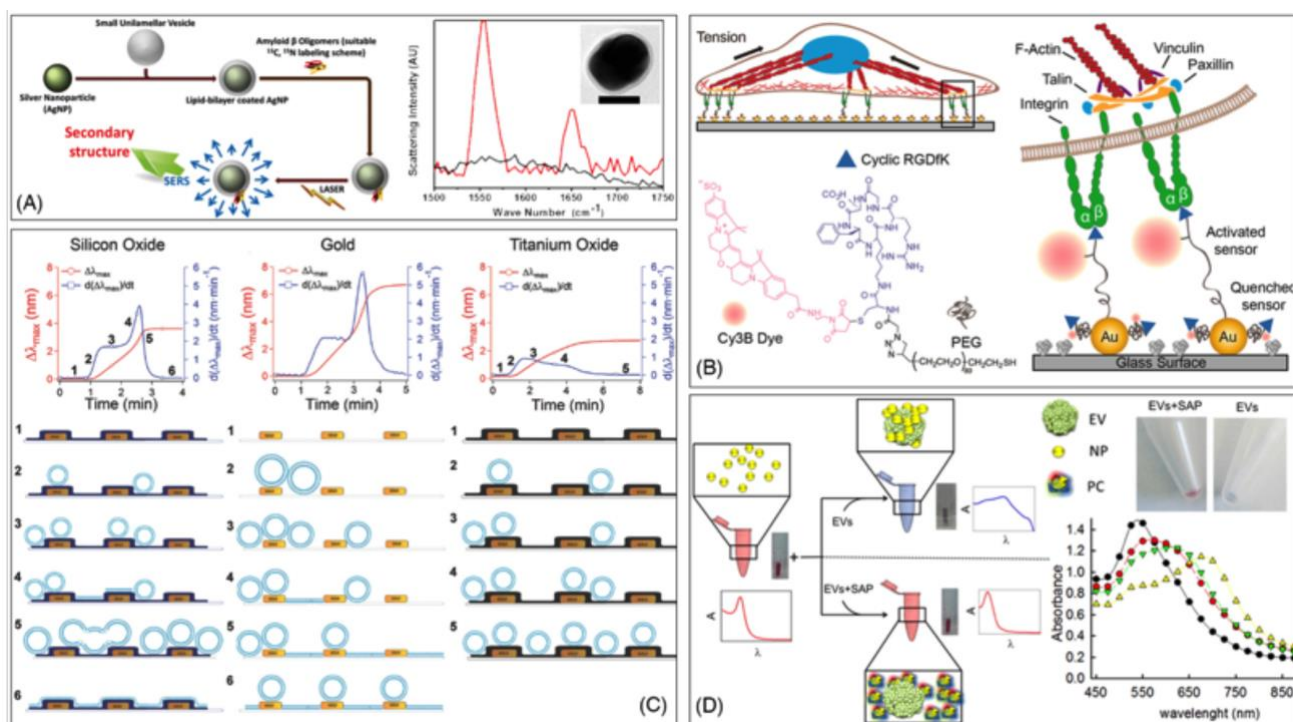


Figure 4 Analytical applications of NP-lipid membrane interactions. *Panel (A)* SERS technique exploiting the spontaneous binding of proteins to lipid bilayer-encapsulated AgNPs to probe lipid membrane-attached oligomers; (left) set-up of the technique (right) TEM micrograph of lipid-coated AgNPs; SERS spectrum of melittin in the presence of AgNPs (black) and lipid-coated AgNPs (red). Adapted with permission from¹²⁷. Copyright (2015) American Chemical Society. *Panel (B)* Molecular tension fluorescence microscopy applied to the investigation of fibroblast cells layered on a substrate with an array of precisely spaced functionalized AuNPs: cartoon summarizing the experimental set-up. Adapted with permission from¹²³. Copyright (2014) American Chemical Society. *Panel (C)* Self-Assembly Formation of Lipid Membranes on Nanoplasmonic Sensor Platforms. Time-resolved extinction maximum wavelength shift measurements (red) and corresponding time derivative (blue) for vesicle adsorption onto (left) silicon oxide-coated nanodisk surface, (center) bare gold nanodisks on glass surface, and (right) titanium oxide-coated nanodisk surface. Adapted with permission from¹²⁴. Copyright (2014) WILEY-VCH Verlag GmbH & Co. KGaA, Weinheim. *Panel (D)* (left) Set-up of the nanoplasmonic assay for probing by eye protein contaminants (single and aggregated exogenous proteins, SAP) in EV preparations; (right) eppendorf tubes containing AuNPs in the presence of EVs (blue) or EVs + SAP (red), highlighting the sensitivity of the assay to EVs protein contaminants; UV-visible absorbance spectra of AuNPs, in the presence of increasing amounts of EVs, highlighting the sensitivity of the assay to EVs concentration. Adapted with permission from¹³⁰. Copyright (2015) American Chemical Society.

section 2; however, it has been demonstrated that electrostatic interactions play a major role also for neutral zwitterionic lipids facing anionic and cationic NPs^{110,111}. In addition, it has been observed that the molecular structure of membrane's lipid components (e.g. saturation degree of hydrophobic chains) represents another factor to take into account, affecting the penetration level of NPs inside the lipid region¹¹². Furthermore, cholesterol, one of the most abundant sterols in real lipid membranes, deeply affects the structure and fluidity of lipid bilayers; moreover, it is involved in the formation of lipid rafts¹¹³, which, for reasons not yet fully understood, increase the extent of NPs-membrane interactions: as an example, Melby et al.¹¹⁴ showed that positively charged AuNPs bind significantly more to phase-segregated bilayers with respect to single phase ones, while Hartono et al.¹¹⁵ associated higher cholesterol concentrations in lipid monolayers to stronger interactions with protein-coated AuNPs, leading to monolayer disruption.

3.4 Biophysics of nano-bio interfaces: NPs-induced membrane modifications

The self-assembled nature and lateral fluidity of plasma membranes determine a capability of the membrane to reorganize and locally and transiently restructure itself in response to biological stimuli. This is the case considering for instance the transient formation of lipid rafts, in relationship with cell trafficking phenomena, or considering ligand (drug) receptor interactions at cell surface, triggering complex biological responses. In this respect, several studies have addressed the effects on NPs on a target lipid membrane upon adhesion. A first effect is the induced lateral phase separation within the target membrane: theoretical studies on cationic NPs have highlighted their tendency to recruit anionic lipids in the adhesion area, determining the formation of phase separated patches within the membrane (See Figure 3B).^{22,116} The alteration of membrane's phase behaviour induced by NPs is a growing research topic, with several studies contributing to building-up a complex picture, which is far from being understood. As an example, the group of Granick¹¹¹ reported a different effect of silica anionic¹¹⁷ and cationic particles on phospholipid membranes, with negative NPs inducing gelation and positive ones provoking fluidification. Considering anionic silica NPs with different size, the group of Zhang et al.¹¹⁸ reported that the gelation, or "freeze effect" on DOPC giant unilamellar vesicles (GUV) is promoted by small NPs (18 nm), while large particles (>78 nm) promote membrane wrapping, significantly decreasing the phospholipid lateral mobility, the release of tension through stress-induced fracture mechanisms results in a microsize hole in the GUVs after interaction. On the other hand, membrane wrapping leads to increased lipid lateral mobility and the eventual collapse of the vesicles. Von White et al.³⁰ registered an increase in the gel-to-liquid crystalline transition temperature of synthetic lipid vesicles induced by the embedding of hydrophobic AuNPs, while Chakraborty et al.¹¹⁹ reported the opposite effect, i.e. phospholipid bilayer softening, due to hydrophobic AuNPs

inclusions; on the other side, recent studies demonstrated that hydrophilic (negatively and positively charged) AuNPs induce the same effect at the nanoscale, promoting the formation of rigidified lipid domains around the NPs' surface, characterized by a reduced lipid motion with respect to the surrounding fluid phase^{21,22,120,121}. Both the induced lateral phase separation on a target membrane and the induced modification of the viscoelastic properties might represent, at the biological level, both biologically relevant signals, activating cell entry pathways, or else might be of relevance in inducing cytotoxic effects (Figure 3 C).

3.5 Analytical Applications of NP-lipid membrane interactions

An interesting research topic related to the interaction of NPs with lipid membranes is its exploitation for analytical purposes. Inorganic NPs are characterized by peculiar properties, making them suitable to provide a readout, generally an optical (fluorescence, scattering) or magnetic signal, which can provide qualitative or quantitative information of different nature. Knowles and coworkers have shown how the spontaneous formation of a supported lipid bilayer on a polystyrene NPs patterned support can be exploited to form membrane regions of high curvature, due to NPs partial wrapping: these areas spontaneously accumulate specific, single-tailed lipids, of higher spontaneous curvature, and can be exploited to monitor the interaction of biomolecules with membrane areas of high curvature¹²²; Liu et al.¹²³ have formed AuNPs patterned surfaces (See Figure 4B), for mechanical tension measurements in living cells. Cho and coworkers¹²⁴ have designed a nanoplasmonic biosensor made of an array of gold, silicon oxide or titanium oxide nanodisks coated with different lipid architectures (See Figure 4C), vesicles arrays, supported lipid bilayers or a coexistence of the two systems, spontaneously formed due to different pathways of interaction between lipid vesicles and the nanodisks of different material: localized surface plasmon resonance experiments detecting a membrane-active peptide highlighted a strong dependence of the interaction between the peptide and the lipid bilayer, depending on the architecture of the lipid scaffold. Limaj et al.¹²⁵ designed an infrared biosensor to monitor the molecular behaviour and dynamics of lipid membranes, based on the adsorption of lipid vesicles on an engineered substrate functionalized with gold nanoantennas for surface enhanced infrared absorption (SEIRA) experiments. Suga et al.¹²⁶ exploited the interaction of hydrophobic (dodecanthiol-modified) AuNPs with phospholipids and phospholipid assemblies, to investigate the behavior of lipid membranes at a molecular length-scale through Surface-Enhanced Raman Spectroscopy (SERS). The same technique is employed by Bhowmik et al.¹²⁷, who exploit the formation of a lipid coating wrapping Silver NPs (AgNPs) to probe through SERS the molecular behavior of protein oligomers spontaneously binding to the lipid coating of AgNPs (this example will be also discussed in section 5) (See Figure 4A). Recently, we have shown that synthetic Giant Unilamellar Vesicles of POPC promote the

clusterization of Turkevich-Frens citrated AuNPs on the lipid membrane itself¹²¹. This phenomenon, which has been investigated by other groups, provokes a modification of the plasmon resonance peak of AuNPs, which is visible also by naked eyes as a colour change of AuNPs dispersion from red to blue^{17,128}. Interestingly, this effect is similarly observed when the same AuNPs challenge biogenic natural vesicles (extracellular vesicles, EVs)^{120,129} and it has been found as strongly dependent on the concentration of EVs and on the presence of protein contaminant. Therefore, an analytical method for EVs has been developed, offering an easy and fast assay for purity and concentration of EVs, based on nonspecific interactions between NPs and lipid membranes^{130–132} (see Figure 4D).

4. Engineering Lipid Assemblies: Inclusion of NPs in Lipid Scaffolds

Depending on their molecular structure and on the environmental conditions, lipids in water self-assemble into very diverse structures, from simple planar lamellar phases, vesicles, to non-lamellar curved bilayered structures (as cubic mesophases)^{133–135}, to inverse monolayered tubular arrangements (as inverse hexagonal mesophases). These different structural arrangements, formed by spontaneous self-assembly, can host hydrophilic-coated NPs in the aqueous regions and/or hydrophobic-coated NPs in the hydrophobic domains. NPs can spontaneously insert in the lipid scaffolds, due to non-specific forces, such as hydrophobic, electrostatic and Van der Waals interactions (see paragraph 2), thus representing a facile approach to obtain a complex hybrid material with controlled structure and defined properties arising from the combination of lipid and NP building blocks. In particular, the inclusion of NPs in lipid scaffolds allows obtaining materials with specific interesting features: (i) the biocompatibility of the lipid scaffold (dependent on its composition) allows envisioning the employment of these hybrid materials for biomedical applications; (ii) the self-organization and phase behavior of lipid mesophases is generally responsive to the inclusion of external species, temperature, hydration and other experimental conditions, which variations can be triggered, in a space and time controlled manner, by external *stimuli* applied to the NPs included in the lipid scaffold (e.g., magnetoliposomes). This is a very interesting opportunity for several applications, for instance the development of drug delivery systems (DDS) with controlled release abilities; (iii) the inclusion and confinement of NPs in lipid scaffolds has the effect to locally concentrate them and impose them a spatial arrangement. This localized NP concentration increase might be of relevance to enhance NP-related signals (for instance optical or MRI readout for diagnostic applications); in addition, the increased concentration, together with a defined structural architecture, might induce peculiar collective properties of NPs, arising from the lipid scaffold-imposed arrangement.

In the following sections we will revise this topic, in particular focusing on the effect of NPs inclusion on the overall features of lipid/NP hybrid materials (4.1), and, subsequently, on applicative examples of NP/lipid hybrids made of NPs included in lamellar (4.2) and non-lamellar (4.3) lipid mesophases.

4.1 NPs inclusion in Lipid Scaffolds: Structural and Physicochemical Effects

The hydrophobic or hydrophilic nature of NPs, which depends on the coating agent, is the key factor in determining the localization in a lipid assembly. Both lamellar (i.e. liposomes, Giant Unilamellar Vesicles) and non-lamellar (i.e. cubic or hexagonal structures) lipid assemblies are characterized by the coexistence of hydrophobic and hydrophilic domains, capable to host NPs of different nature. In all NPs-lipid hybrids, the inclusion of NPs in the lipid architecture affects the physico-chemical and structural properties of the lipid scaffold, modifying for instance the fluidity and bending properties of the membrane, its local thickness, the phase behavior and the viscoelastic properties. For instance, it has been shown that the inclusion of hydrophobic superparamagnetic iron oxide NPs (SPIONs) in the lipid membrane of DPPC liposomes increases the average thickness of the membrane and modifies the orientation of the phospholipid chains, affecting the lipid melting temperature^{136,137}. In addition, depending on the chemical nature of hydrophobic NPs embedded in a lipid bilayer, they can either stabilize or destabilize the lipid ordering, causing opposite effects on the phase behavior of the lipid scaffold; it has been shown that 4 and 5.7 nm AgNPs³¹ increase the fluidity of the membrane, reducing the degree of ordering of the lipid tails, while 5 nm maghemite NPs²⁹ increase membrane rigidity. Finally, the inclusion of nanoparticles can also modify the final structure of the bilayer: for instance, a Cryo-TEM investigation of Chen et al. on liposomes containing hydrophobic SPIONs has highlighted the formation of liposomes' aggregates with SPIONs clusters acting as bridging agents (See Figure 5A-B). These local perturbations highlight that some structural rearrangement of a planar lipid membrane can be possible preserving the overall lipid mesophase architecture; however, as reported by Briscoe et al.⁴⁰, significant amounts of NPs inclusion might promote, for defined lipid compositions and specific temperature/pressure conditions, a phase transition from lamellar to hexagonal mesophases. In general, as already pointed out in section 2, the inclusion of NPs in a planar bilayer increases the frustration packing energy of the lipid molecules eventually promoting the re-organization in a different mesophase, characterized by a more negative curvature; the mismatch between the equilibrium curvature and the perturbed arrangement due to NP inclusion, favors the transition to a more thermodynamically stable structure.

These examples highlight how the effect of NPs on lipid membranes is variable, but possibly predictable, on the basis of minimum energy considerations; therefore, the physico-chemical properties of the target lipid membrane and of the NPs to be inserted in the lipid scaffold can be tuned in order to

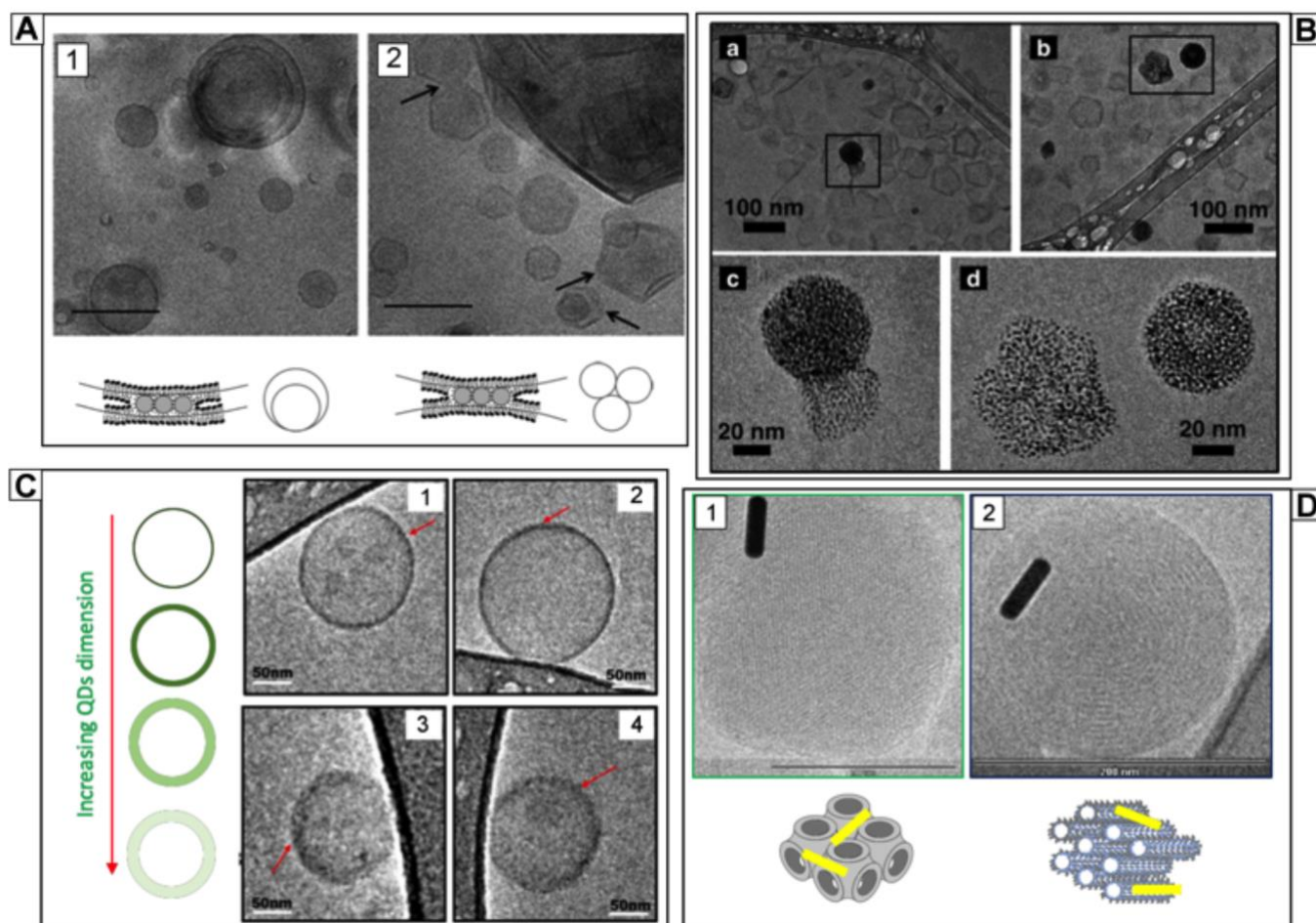


Figure 5 Cryo-Microscopies of Lamellar and Non-Lamellar Lipid membranes assembled with hydrophobic NPs. *Panel (A)* Cryo-TEM images highlighting the structural changes induced by hydrophobic SPIONs interacting with liposomes: on the left, TEM image showing liposomes arranged in a multiwalled configuration with SPIONs bridging; on the right, TEM image of liposomes' aggregates bridged by SPIONs clusters embedded in the bilayer. Adapted with permission from Ref.²⁹. Copyright (2010) American Chemical Society. *Panel (B)* DPPC liposomes decorated with dodecanethiol-capped AuNPs shown at different magnifications. Adapted with permission from Ref.²⁸. Copyright (2017) American Chemical Society. *Panel (C)* TEM images of POPC/POPE liposomes assembled with Quantum Dots (QDs) of different sizes embedded in the bilayer. The size increase of QDs (from 1 to 4 progressively) increases the perturbation of the lipid membrane: lipid membrane appears sharp when small QDs are included (1 and 2), while with the larger ones the membrane becomes fuzzier (3 and 4). Reproduced from Ref.¹⁵⁰ with permission from The Royal Society of Chemistry. *Panel (D)* Cryo-SEM of Non-Lamellar mesophases interacting with Au NRs. On the left Phytantriol cubic mesophase, on the right Phytantriol hexagonal mesophase, both assembled with Au NRs. Adapted with permission from Ref.¹⁵⁶. Copyright (2012) American Chemical Society.

1 modify the behavior of the membrane in a desired manner
 2 engineering the system for its final purpose.
 3
 4 **4.2 Applications of NPs/Lamellar Lipid Assemblies Hybrids**
 5 Among hybrid nanostructures where NPs are included in
 6 lamellar assemblies, particularly relevant are
 7 magnetoliposomes (MLs), where hydrophobic SPIONs are
 8 included in the lipid bilayers of lipid vesicles^{138–140}. Their
 9 responsivity to static (SMF) and alternating magnetic fields
 10 (AMF) makes MLs good candidates in nanomedicine as DDS¹⁴¹
 11 able to release drugs confined in the lumen of liposomes in a
 12 time and space controlled manner, upon application of external
 13 stimuli^{142,143}. Despite their potentiality, the inclusion of small
 14 NPs in the bilayer can be exploited only for drug delivery
 15 purposes, while generally, no bulk heating effect can be induced
 16 by small NPs subjected to AMFs, as shown in several studies¹⁴⁴
 17 therefore, they cannot be applied in hyperthermia therapies
 18 for the thermal ablation of cells; however, as reported by

Corato et al.¹⁴⁵, using hydrophilic SPIONs loaded in the vesicles' lumen combined with a photosensitizer, results in a synergistic effect, observed both *in vitro* and *in vivo*, making this strategy, exploiting a multifunctional nanomaterial, very promising for therapeutic applications. Recently, MLs decorated both with hydrophobic and hydrophilic SPIONs have been shown to release on-demand hydrophilic or hydrophobic payloads, depending on the frequency and application time of an AMF.¹²⁷ Besides SPIONs, hydrophobic AuNPs were recently used¹⁴⁶ to build-up photoresponsive and thermosensitive hybrid liposomes. In addition, multifunctional hybrid liposomes containing magneto-plasmonic nanoparticles (SPIONs@Au), merging the possibility to combine hypothermic and photothermal treatments were recently shown^{147,148} for image-guided delivery of anti-HIV drugs to the brain: generally, the successful delivery of antiretroviral drugs to the brain is limited due to the presence of the blood–brain barrier (BBB); in this case the authors reported an enhanced BBB transmigration efficiency under AMF without its disruption; moreover, the

treatment of HIV virus with multifunctional liposomes⁵⁷ successfully reduced the viral replication.⁵⁸ Several studies have addressed the inclusion of quantum dots⁵⁹ in lipid assemblies: despite their unique optical properties, they⁶⁰ are characterized by significant acute cytotoxic effects. With the⁶¹ aim to realize a contrast agent for imaging applications^{138,149,150}, several studies have shown that the confinement of CdSe dots⁶² in lipid bilayers increases their biocompatibility, while⁶⁴ preserving their fluorescence features, making the system more⁶⁵ suitable for biomedical applications (See Figure 5 C).⁶⁶

4.3 Applications of NPs/Non-Lamellar Lipid Assemblies Hybrids

As anticipated in section 2, the inclusion of NPs into non⁶⁷ lamellar lipid assemblies mostly affects the structure of the⁷⁰ mesophase, in terms of the lattice parameter and⁷¹ consequently, of the diameter of the nanochannels and amount⁷² of water contained in the lipid architecture. If the size of NPs is⁷³ similar or smaller than the lattice parameter, NPs can be easily⁷⁴ encapsulated in the architectures. Venugopala et al.⁷⁵ investigated the encapsulation of hydrophilic Silica NPs of 8 nm⁷⁶ diameter in monolinolein mesophase: in this case, the NPs⁷⁷ were too large to be encapsulated in the nanochannels (of 3.8 nm⁷⁸ diameter); nevertheless, the addition of NPs determined⁷⁹ the overall dehydration of the lipid scaffold, eventually causing⁸⁰ for high concentration, the transition of the assembly geometry⁸¹ to a gyroid cubic structure (Ia3d). The authors interpret this⁸² behavior considering that, since the energy cost to include the⁸³ NPs in the nanochannels is extremely high (above 100 k_BT), the⁸⁴ NPs tend to minimize their interfacial energy, aggregating along⁸⁵ the grain boundaries of the mesophase, similarly to what⁸⁶ reported concerning lamellar structures¹⁵¹. The same authors⁸⁷ investigated also the structural features of monolinolein⁸⁸ mesophases loaded with hydrophilic SPIONs. Upon application⁸⁹ of a SMF, a reorganization of the lipid domains along the⁹⁰ direction of the field^{152,153} was found, highlighting how the⁹¹ responsiveness of SPIONs to magnetic fields can be exploited to⁹² induce structural modifications in the whole lipid mesophase.⁹³ This effect has been applied for instance to control the release⁹⁴ of drugs confined in the lipid mesophases¹⁵² or, as the same⁹⁵ authors reported¹⁵⁴, for the application in optical memory⁹⁶ storage.

The inclusion of hydrophobic NPs in non-lamellar mesophases⁹⁷ can be easily achieved exploiting the hydrophobic interactions⁹⁸ that spontaneously drive the NPs localization in the⁹⁹ hydrophobic regions of the self-assembly. However, also in this¹⁰⁰ case, the size of NPs is of paramount importance, to avoid the¹⁰¹ disruption of the lipid scaffold. Recently, the inclusion of¹⁰² hydrophobic SPIONs into 1-monoolein diamond cubic phase¹⁰³ was reported, highlighting that the amount of included NPs,¹⁰⁴ together with temperature, control the phase transition from¹⁰⁵ cubic to hexagonal phase. Since this transition is accompanied¹⁰⁶ by a significant dehydration of the mesophase, the structural¹⁰⁷ rearrangement is accompanied by the release of most of the¹⁰⁸ water content of the nanochannels. This thermoresponsive¹⁰⁹ hybrid material was also found to be responsive to AMF,¹¹⁰ representing, therefore, a promising system for the delivery of

hydrophilic drugs in a time and space-controlled manner.³³ Recently, it was shown that this thermotropic effect of liquid¹¹¹ crystalline phases loaded with hydrophobic NPs is a general¹¹² phenomenon, highlighted e.g. also by cubic mesophases¹¹³ formed of phytantriol and hydrophobic AuNPs.²⁰ Very few examples in the literature address the inclusion of¹¹⁴ non-spherical NPs in non-lamellar lipid assemblies: Boyd et al.¹⁵⁵ reported on hydrophobic NRs included in phytantriol, selachyl¹¹⁵ alcohol and monoolein lipid mesophases, with the aim to build-¹¹⁶ up photo-responsive hybrid materials (See Figure 5D). The¹¹⁷ authors investigate the effect of NRs on the cubic mesophases,¹¹⁸ highlighting a slight reduction in the phase transition¹¹⁹ temperature and in the lattice parameter. Interestingly,¹²⁰ similarly to spherical hydrophobic NPs, gold NRs shift the cubic-¹²¹to-hexagonal boundaries to lower temperature¹⁵⁶. For¹²² hexosomes of selachyl alcohol, it was shown that the lattice¹²³ parameter or water volume fraction^{26,27} are not affected by the¹²⁴ presence of AuNRs; the authors suggest that NRs are positioned¹²⁵ along the direction of hexosomes, but, due to their large sizes¹²⁶ (55.5 nm in length and 16 nm in width) they are in close¹²⁷ proximity of the lipid bilayer, without being efficiently included¹²⁸ inside it. Nevertheless, the application of a NIR laser on the¹²⁹ hybrid structure promoted the phase transition from cubic to¹³⁰ hexagonal phase, similarly to what observed with the¹³¹ application of AMF on monoolein-SPIONs hybrids.

5. Surface Engineering of Inorganic NPs: Functionalization of NPs with a Lipid Coating

Recently, several research groups have addressed the¹³² functionalization of inorganic NPs or clusters of NPs with lipids¹³³ to form lipid-coated NPs with a supported lipid bilayer (SLB and¹³⁴ liposomes³). The validity of this approach is twofold: first, a lipid¹³⁵ coating of appropriate composition might strongly improve the¹³⁶ biocompatibility of inorganic NPs: this is particularly critical for¹³⁷ the very toxic quantum dots. The second advantage is the¹³⁸ increased dispersibility in body fluids and improved¹³⁹ pharmacokinetic properties. As a matter of fact, without a¹⁴⁰ proper coating, bare NPs introduced by parenteral¹⁴¹ administration, are rapidly opsonized and removed by¹⁴² phagocytes from the blood stream⁵⁴ and accumulated in liver¹⁴³ and spleen^{157,158}, often causing oxidative stress^{159,160}.

Although this could be even convenient for those treatments¹⁴⁴ where the desired aim is to modulate local immune¹⁴⁵ responses¹⁶¹, it is worth considering the use of a capping agent¹⁴⁶ that prevents leakage of the drug, protects the carrier from¹⁴⁷ degrading enzymes, and shields them from the immune system¹⁴⁸ avoiding side effects^{162,163}. Among several potential capping¹⁴⁹ systems, lipid bilayers are especially advantageous¹⁶⁴ for several¹⁵⁰ reasons: (i) the escape from endosomal vesicles of the¹⁵¹ nanomaterial and successful reaching of its biological target,¹⁵² upon endocytic uptake, is strongly favoured in the presence of¹⁵³ a lipid coating, improving the ability of NPs to passively¹⁵⁴ permeate to the inner core of the cell^{165,166}; (ii) the presence of¹⁵⁵ a lipid coating is helpful in preventing NPs aggregation in¹⁵⁶ biological environment; (iii) lipid coating is highly tuneable in

composition (for instance PEGylated lipids, to further improve nanoparticle pharmacokinetic properties¹⁶⁷, can be easily incorporated, as well as cholesterol, added as a controlling fluidity agent) and can be easily functionalized and designed to match the specific requirements of the desired application¹⁶⁸. As introduced in section 2, the achievement of such coating depends on the size of the NP to be coated and on the viscoelastic properties of the membrane. Generally, relatively large NPs, imposing a low curvature to the target membrane, can be successfully completely wrapped and coated by a lipid membrane, while small particles need to be wrapped and coated as clusters. In the following sections we will review the most relevant examples and applications of lipid-coated inorganic nanoparticles, considering one by one the different types of nanoparticles, Silica NPs (5.1), Gold and Silver NPs (5.2) and Iron Oxide NPs (5.3).

5.1 Lipid-coated Silica NPs

Leveraging the pioneering works of Rapuano's groups^{171,172}, over the last years several research groups have addressed the decoration of silica nanoparticles with SLBs¹⁷³. Recently Mousseau et al. showed an example of fluorescent silica NPs covered by a pulmonary surfactant Curosurf®. They found that a complete SLB coverage of silica nanoparticles is obtained only through sonication, which disrupts lipid vesicles and promotes

full wrapping of the NPs. *In vitro* assays confirmed that the presence of the SLB mitigated the particle toxicity and improved internalization rates¹⁷⁴.

Tada and co-workers tested the impact of a lipid coating (using different types of lipid bilayers) on the cytolocalization of silica NPs prepared with methylene blue, for applications in Photodynamic Therapy (PDT)^{175,176}.

Mackowiak et al.¹⁷⁷ showed an example of mesoporous silica NPs surrounded by a cationic DOPC/DOTAP SLB with targeting ligands on the surface of the nanoconstruct and a photosensitizer molecule covalently attached to the surface of mesoporous silica NPs, for controlled and targeted drug delivery applications. In this case, the presence of the SLB coating was also aimed at improving the capability of the system to retain a drug inside the mesoporous structure of NPs before photoactivation to induce the release of the cargo.

An alternative route to obtain controlled release of drugs from lipid-coated mesoporous silica NPs, based on the use of thermo-responsive lipids, was recently presented by Zhang et al.: they combined the high drug loading capacity of mesoporous silica NPs with the thermal responsiveness of a mixture of lipids, DPPC/DSPE/Chol/DSPE-PEG2000, allowing the possibility to release on-demand the payload at hyperthermia temperature, circumventing the premature leakage at physiological temperature¹⁷⁸ (See Figure 6C).

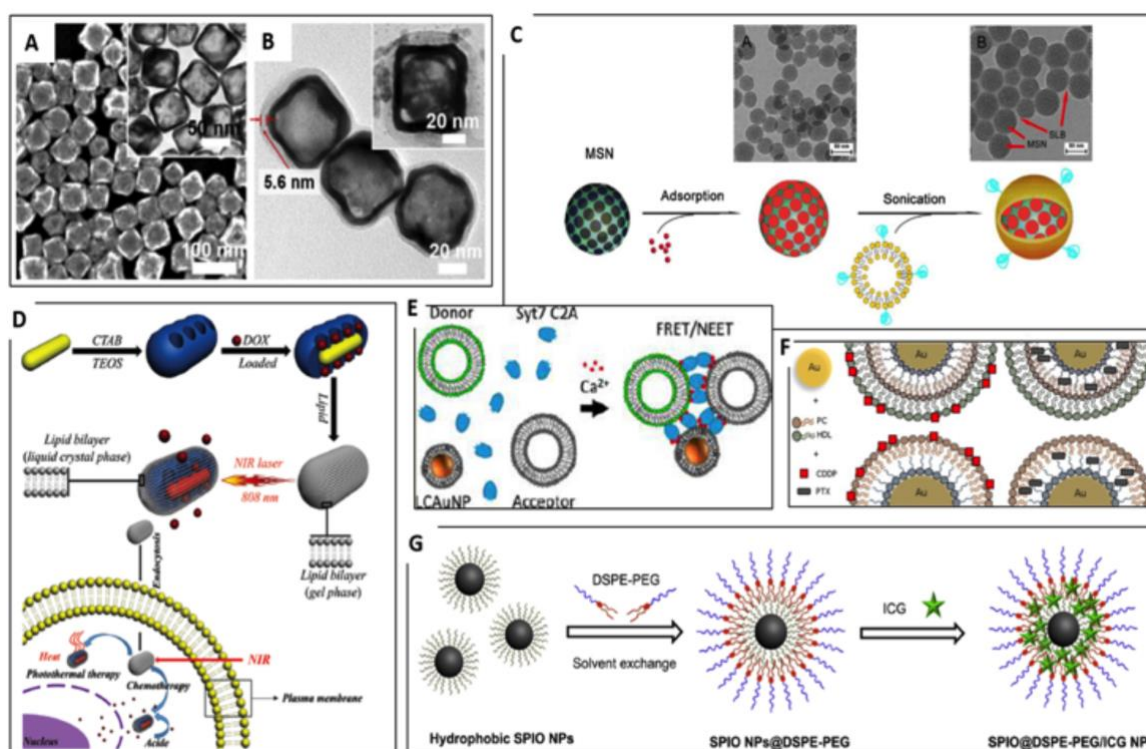


Figure 6 Lipid-coated NPs. Panel (A-B) TEM images of bare Au nanocages (A) and the same nanocages covered by a lipid bilayer (B) used as nanovaccine for cancer immunotherapy. Reprinted with permission from ref.¹⁸⁷ © Elsevier; Panel (C) Schematic overview of the procedure for the fabrication of doxorubicin (DOX)-loaded SLB-mesoporous silica NPs. The thermal responsiveness of the lipids circumvents the premature leakage of the payload. The insets show the related TEM images. Adapted and reprinted with permission from ref.¹⁷⁸ © Elsevier; Panel (D) Schematic illustration of the fabrication process of DOX-AuNR@mSiO₂ covered by a lipid bilayer and the corresponding NIR laser-controlled intracellular DOX release. Reprinted with permission from ref.¹⁹² © RSC; Panel (E) Model of the Ca²⁺-dependent liposome and lipid-coated AuNPs clustering in presence of synaptotagmin (SyT). Reprinted with permission from ref.¹⁸⁵ © ACS; Panel (F) Conceptual scheme of lipid-coated gold carriers for the release of paclitaxel and cisplatin. Reprinted with permission from ref.¹⁸³ © Elsevier; Panel (G) Schematic illustration of the preparation protocol of SPION@DSPE-PEG loaded with indocyanine green. Reprinted with permission from ref.¹⁹³ © Elsevier.

5.2 Lipid-coated Gold and Silver NPs

Taking advantage of their antimicrobial properties, AgNPs have been widely used in the last decades both in industrial and in biomedical application^{179–181}. Furthermore, due the localized surface plasmon resonance (LSPR) of AgNPs, they can be exploited for the development of biosensors. For this purpose, Bhowmik et al.¹²⁷ developed a method to determine the conformation of membrane-bound proteins: unlike conventional SERS, that requires immobilization of molecules, they exploit the spontaneous binding of proteins to lipid bilayer-coated AgNPs. In this way, they probed the behavior of membrane-attached oligomers of Amyloid- β 40 (A β 40), whose conformation is of relevance in Alzheimer's disease. AuNPs are the most widely studied inorganic NPs, thanks to their facile synthetic and functionalization routes, and their plasmonic properties that can be harnessed in a plethora of applications ranging from optical imaging, spectroscopy and photothermal therapy. Du et al. formed a liposomes-AuNPs hybrid system as a vector for nucleic acids, for applications in gene therapy¹⁸². England and co-workers^{183,184} (See Figure F) prepared AuNPs functionalized with multiple layers (two or three) of phosphatidylcholine, alkanethiol, high density lipoprotein and phosphatidylcholine/alkanethiol for the delivery of hydrophobic and hydrophilic drugs for the treatment of solid tumours. By exploiting the optical properties of AuNPs, Reed et al. developed a novel hybrid for sensitive detection of proteins based on apposition and aggregation of liposomes induced by Ca^{2+} ions using Förster resonance energy transfer (FRET) assays¹⁸⁵ (See Figure E). Wang et al. recently proposed a novel approach to overcome the low delivery efficiency of plasmids by condensing them on peptide-modified AuNPs, successively covered with a mixture of phospholipids¹⁸⁶. In addition to spherical NPs, liposomes-coated gold nanocages¹⁸⁷ (See Figure 6A–B) have been reported as possible nanovaccines for cancer immunotherapy: the authors demonstrated that the hybrid carrier exhibited enhanced antitumor effects, inhibiting tumour growth in lung metastasis models. In addition, lipid-coated hollow gold nanoshells have been recently developed for synergistic chemotherapy and photothermal therapy for the treatment of pancreatic cancer¹⁸⁸. By taking advantage of the unique structure of hollow gold nanoshells, the authors successfully demonstrated the co-delivery of two drugs, one loaded in the lipid bilayer and the other one loaded in the hydrophilic interior of the nanoshell. Furthermore, the possibility to extend lipid coverage to Au NRs has been recently explored. Recent studies have addressed the functionalization of Au NRs with a phospholipid bilayer composed of POPC¹⁸⁹ and, more recently, DMPC¹⁹⁰, to increase biocompatibility and bioavailability of NRs. In addition, lipid-capped Au NRs (obtained with DPPC vesicles containing lipids with a thiol headgroup) have been demonstrated to be suitable for label-free biosensors¹⁹¹ for the detection of lipophilic drugs in aqueous solutions or lipopeptides in serum. Finally, moving to more complex architecture, Han et al.¹⁹² (See Figure 6D) demonstrated the possibility to use silica and phospholipids to

cover Au NRs, coupling the photothermal and thermo-responsive properties in the same nanoplatform.

5.3 Lipid-coated Iron Oxide NPs

SPIONs are among the most attractive NPs for biomedical applications, ranging from applications in MRI to responsive nanocarriers for drug delivery to therapeutic applications in hyperthermia (See Figure G). Bao et al.¹⁹³ synthesized DSPE-PEG coated SPIONs loaded with indocyanine green molecules as superparamagnetic carriers capable to easily accumulate in tumours sites and act as biodegradable nanotheranostic agents. In the emerging field of nanovaccines, the group of Ruiz-de-Angulo¹⁹⁴ presented a biocompatible multifunctional system designed to both act as delivery vehicle and radiotracer for PET/SPECT imaging: using lipid-coated magnetite nanoparticles, they efficiently included in the construct $^{67}\text{Ga}^{3+}$ as radiotracer, plus an antigen and an adjuvant. *In vivo* imaging highlighted the efficient targeting capability of the system and cell uptake. Recently, the same authors presented bacteria-mimicking NPs, that is, a similar construct (i.e., lipid coated magnetite nanoparticles), coated with lipooligosaccharides, which efficiently act as adjuvants¹⁹⁵ for application in cancer vaccine field.

Enveloping a magnetic iron oxide core with a lipid shell facilitates bioconjugation, biocompatibility, and delivery, as well reported by Wang et al.¹⁹: in their work they provide a general solution for coating iron oxide and other metal oxides with a simple mixing in water, facilitating applications in biosensing, separation, and nanomedicine.

A multifunctional system for dual imaging (fluorescence and MRI) of hepatocellular carcinoma was reported by Liang et al.¹⁹⁶: through the thin film hydration method, they covered magnetite NPs previously conjugated with a NIR fluorescent dye; the lipid bilayer was decorated with a polymer targeting tumour hepatocytes, able to steer the carrier to the specific site. By flow cytometry and confocal laser scanning microscopy they assessed the specific cellular uptake, followed by *in vivo* tests on tumor-bearing mice.

6. Conclusions

In this contribution we have reviewed the latest developments concerning the interaction of NPs with amphiphilic bilayers arranged in lamellar and non-lamellar mesophases.

This area is a very lively research field, where efforts are motivated by several scientific purposes. First of all, the application of nanostructured materials in the biomedical field requires a precise knowledge of the nano-bio-interface: bilayered synthetic assemblies are a very convenient and simple platform to elucidate the interactions with cell membranes and internalization of nanomedical devices. In addition, the design of smart nanostructured hybrid devices, where NPs are included in soft matter assemblies to contribute new properties and modulate their phase diagram is a very relevant and active research field. Related to this latter area is the use of lipid

- bilayers as coating shells for inorganic nanoparticles, to improve their biocompatibility and interaction with cell membranes. In all cases, the mechanistic understanding of the material thermodynamic parameters involved in this interaction and their dependence on the physico-chemical features both of the nanomaterials and of the bilayers, are a necessary prerequisite to engineer soft matter hybrids and formulate NPs with potential applications in the biomedical field. Soft Matter science represents therefore the central discipline, whose scientific and methodological approaches will be more and more pivotal to contribute to meaningful progresses in this field. If the promises held by this approach will be fulfilled in the next decades, many of the current hurdles that nowadays hamper the full development of nanomedicine can be overcome.
- Finally, a precise knowledge of the above-mentioned features allows engineering NPs to probe the properties of complex bilayer assemblies, both of natural and synthetic origin. This is a very exciting and promising area, where fundamental and applied efforts should be directed in the next decade.
- ## Conflicts of interest
- There are no conflicts to declare
- ## Acknowledgements
- Costanza Montis acknowledges the European Union's Horizon 2020 programme (evFOUNDRY grant agreement 801367). All the authors thank CSGI for financial support.
- ## References
- 1 C. Lu, Y. Liu, Y. Ying and J. Liu, *Langmuir*, 2017, **33**, 630–637.
 - 2 P.-J. J. Huang, F. Wang and J. Liu, *Langmuir*, 2016, **32**, 2458–2463.
 - 3 X. Wang, X. Li, H. Wang, X. Zhang, L. Zhang, F. Wang and J. Liu, *Langmuir*, 2019, **35**, 1672–1681.
 - 4 F. Wang and J. Liu, *J. Am. Chem. Soc.*, 2015, **137**, 11736–11742.
 - 5 F. Wang and J. Liu, *Nanoscale*, 2013, **5**, 12375.
 - 6 Y. Liu and J. Liu, *Nanoscale*, 2017, **9**, 13187–13194.
 - 7 V. C. Sanchez, A. Jachak, R. H. Hurt and A. B. Kane, *Chem. Res. Toxicol.*, 2012, **25**, 15–34.
 - 8 R. Koole, M. M. van Schooneveld, J. Hilhorst, K. Castermans, D. P. Cormode, G. J. Strijkers, C. de Mello Donegá, D. Vanmaekelbergh, A. W. Griffioen, K. Nicolay, A. Fayad, A. Meijerink and W. J. M. Mulder, *Bioconjug. Chem.*, 2008, **19**, 2471–2479.
 - 9 A. H. Bahrami, M. Raatz, J. Agudo-Canalejo, R. Michel, E. Curtis, C. K. Hall, M. Gradzielski, R. Lipowsky and T. R. Weikel, *Adv. Colloid Interface Sci.*, 2014, **208**, 214–224.
 - 10 S. Dasgupta, T. Auth and G. Gompper, *J. Phys. Condens. Matter*, 2017, **29**, 373003.
 - 11 X. Chen, F. Tian, X. Zhang and W. Wang, *Soft Matter*, 2013, **9**, 7592.
 - 12 Y. Roiter, M. Ornatska, A. R. Rammohan, J. Balakrishnan, D. R. Heine and S. Minko, *Nano Lett.*, 2008, **8**, 941–944.
 - 13 C. Contini, M. Schneemilch, S. Gaisford and N. Quirke, *J. Exp. Nanosci.*, 2018, **13**, 62–81.
 - 14 Q. Mu, G. Jiang, L. Chen, H. Zhou, D. Fourches, A. Tropsha and B. Yan, *Chem. Rev.*, 2014, **114**, 7740–7781.
 - 15 S. Dasgupta, T. Auth and G. Gompper, *Nano Lett.*, 2014, **14**, 687–693.
 - 16 A. H. Bahrami, *Soft Matter*, 2013, **9**, 8642.
 - 17 F. Wang and J. Liu, *Nanoscale*, 2015, **7**, 15599–15604.
 - 18 F. Wang, D. E. Curry and J. Liu, *Langmuir*, 2015, **31**, 13271–13274.
 - 19 F. Wang, X. Zhang, Y. Liu, Z. Y. W. Lin, B. Liu and J. Liu, *Angew. Chemie Int. Ed.*, 2016, **55**, 12063–12067.
 - 20 X. Liu, X. Li, W. Xu, X. Zhang, Z. Huang, F. Wang and J. Liu, *Langmuir*, 2018, **34**, 6628–6635.
 - 21 J. Liu, *Langmuir*, 2016, **32**, 4393–4404.
 - 22 T. Pfeiffer, A. De Nicola, C. Montis, F. Carlà, N. F. A. van der Vegt, D. Berti and G. Milano, *J. Phys. Chem. Lett.*, 2019, **10**, 129–137.
 - 23 M. Schulz, A. Olubummo and W. H. Binder, *Soft Matter*, 2012, **8**, 4849.
 - 24 C. F. Su, H. Merlitz, H. Rabbel and J. U. Sommer, *J. Phys. Chem. Lett.*, 2017, **8**, 4069–4076.
 - 25 R. C. Van Lehn and A. Alexander-Katz, *Soft Matter*, 2014, **10**, 648–658.
 - 26 M. Mendoza, C. Montis, L. Caselli, M. Wolf, P. Baglioni and D. Berti, *Nanoscale*, 2018, **10**, 3480–3488.
 - 27 M. Mendoza, L. Caselli, C. Montis, S. Orazzini, E. Carretti, P. Baglioni and D. Berti, *J. Colloid Interface Sci.*, 2019, **541**, 329–338.
 - 28 M. R. Preiss, A. Hart, C. Kitchens and G. D. Bothun, *J. Phys. Chem. B*, 2017, **121**, 5040–5047.
 - 29 Y. Chen, A. Bose and G. D. Bothun, *ACS Nano*, 2010, **4**, 3215–3221.
 - 30 G. Von White, Y. Chen, J. Roder-Hanna, G. D. Bothun and C. L. Kitchens, *ACS Nano*, 2012, **6**, 4678–4685.
 - 31 G. D. Bothun, *J. Nanobiotechnology*, 2008, **6**, 1–10.
 - 32 Z. A. Almsheerqi, T. Landh, S. D. Kohlwein and Y. Deng, in *International Review of Cell and Molecular Biology*, Elsevier Inc., 1st edn., 2009, vol. 274, pp. 275–342.
 - 33 D. P. Chang, J. Barauskas, A. P. Dabkowska, M. Wadsäter, F. Tiberg and T. Nylander, *Adv. Colloid Interface Sci.*, 2015, **222**, 135–147.
 - 34 W. K. Fong, R. Negrini, J. J. Vallooran, R. Mezzenga and B. J. Boyd, *J. Colloid Interface Sci.*, 2016, **484**, 320–339.
 - 35 I. W. Hamley, *Angew. Chemie*, 2003, **115**, 1730–1752.
 - 36 G. C. Shearman, O. Ces, R. H. Templer and J. M. Seddon, *J. Phys. Condens. Matter*, 2006, **18**, S1105–S1124.
 - 37 C. M. Beddoes, C. P. Case and W. H. Briscoe, *Adv. Colloid Interface Sci.*, 2015, **218C**, 48–68.
 - 38 E. Venugopal, S. K. Bhat, J. J. Vallooran and R. Mezzenga, *Langmuir*, 2011, **27**, 9792–9800.
 - 39 M. Slezak, D. Nieciecka, A. Joniec, M. Pękala, E. Gorecka, M. Emo, M. J. Stébé, P. Krysiński and R. Bilewicz, *ACS Appl. Mater. Interfaces*, 2017, **9**, 12889.
 - 40 J. M. Bulpett, T. Snow, B. Quignon, C. M. Beddoes, T.-Y. D.

- 1 Tang, S. Mann, O. Shebanova, C. L. Pizze, N. J. Terrill, S. A58
- 2 Davis and W. H. Briscoe, *Soft Matter*, 2015, **11**, 8789–80059 63
- 3 41 C. M. Beddoes, J. Berge, J. E. Bartenstein, K. Lange, A. J. 60
- 4 Smith, R. K. Heenan and W. H. Briscoe, *Soft Matter*, 2016, 61
- 5 **12**, 6049–6057. 62 64
- 6 42 C. Montis, B. Castroflorio, M. Mendoza, A. Salvatore, D. 63
- 7 Berti and P. Baglioni, *J. Colloid Interface Sci.*, 2015, **449**, 64 65
- 8 317–326. 65
- 9 43 K. L. Chen and G. D. Bothun, *Environ. Sci. Technol.*, 2014, 66 66
- 10 **48**, 873–880. 67
- 11 44 M. Henriksen-Lacey, S. Carregal-Romero and L. M. Liz- 68 67
- 12 Marzán, *Bioconjug. Chem.*, 2017, **28**, 212–221. 69
- 13 45 E. Rascol, J.-M. Devoisselle and J. Chopineau, *Nanoscale*, 70 68
- 14 2016, **8**, 4780–4798. 71 69
- 15 46 E. Blanco, H. Shen and M. Ferrari, *Nat. Biotechnol.*, 2015, 72
- 16 **33**, 941–951. 73 70
- 17 47 P. Falagan-Lotsch, E. M. Grzincic and C. J. Murphy, *Proc.* 74
- 18 *Natl. Acad. Sci.*, 2016, **113**, 13318–13323. 75 71
- 19 48 C. J. Murphy, A. M. Vartanian, F. M. Geiger, R. J. Hamers, 76
- 20 Pedersen, Q. Cui, C. L. Haynes, E. E. Carlson, R. Hernandez 77
- 21 R. D. Klapser, G. Orr and Z. Rosenzweig, *ACS Cent. Sci.*, 2013, 78
- 22 **1**, 117–123. 79 72
- 23 49 L. J. Fox, R. M. Richardson and W. H. Briscoe, *Adv. Colloid* 80 73
- 24 *Interface Sci.*, 2018, **257**, 1–18. 81
- 25 50 S. Wilhelm, A. J. Tavares, Q. Dai, S. Ohta, J. Audet, H. F. 82
- 26 Dvorak and W. C. W. Chan, *Nat. Rev. Mater.*, 2016, **1**, 83 74
- 27 16014. 84
- 28 51 D. Bobo, K. J. Robinson, J. Islam, K. J. Thurecht and S. R. 85 75
- 29 Corrie, *Pharm. Res.*, 2016, **33**, 2373–2387. 86
- 30 52 Y. H. Choi and H. K. Han, *J. Pharm. Investig.*, 2018, **48**, 43–87
- 31 60. 88 76
- 32 53 J. M. Caster, A. N. Patel, T. Zhang and A. Wang, *Wiley* 89
- 33 *Interdiscip. Rev. Nanomedicine Nanobiotechnology*, , 90
- 34 DOI:10.1002/wnan.1416. 91 77
- 35 54 C. D. Walkey and W. C. W. Chan, *Chem. Soc. Rev.*, 2012, **41**, 92
- 36 2780–2799. 93
- 37 55 A. E. Nel, L. Mädler, D. Velegol, T. Xia, E. M. V. Hoek, P. 94 78
- 38 Somasundaran, F. Klaessig, V. Castranova and M. 95
- 39 Thompson, *Nat. Mater.*, 2009, **8**, 543–557. 96
- 40 56 S. Zhang, H. Gao and G. Bao, *ACS Nano*, 2015, **9**, 8655– 97 79
- 41 8671. 98
- 42 57 N. S. Bhise, J. Ribas, V. Manoharan, Y. S. Zhang, A. Polini, 99
- 43 Massa, M. R. Dokmeci and A. Khademhosseini, *J. Control* 100 80
- 44 *Release*, 2014, **190**, 82–93. 101
- 45 58 G. Rossi and L. Monticelli, *Biochim. Biophys. Acta -* 102 81
- 46 *Biomembr.*, 2016, **1858**, 2380–2389. 103
- 47 59 V. Pillay, K. Murugan, Y. E. Choonara, P. Kumar, D. 104
- 48 Bijukumar and L. C. du Toit, *Int. J. Nanomedicine*, 2015, **10**, 105 82
- 49 2191. 106
- 50 60 I. Canton and G. Battaglia, *Chem. Soc. Rev.*, 2012, **41**, 27107
- 51 61 M. Calero, L. Gutiérrez, G. Salas, Y. Luengo, A. Lázaro, P. 108 83
- 52 Acedo, M. P. Morales, R. Miranda and A. Villanueva, 109
- 53 *Nanomedicine Nanotechnology, Biol. Med.*, 2014, **10**, 73310 84
- 54 743. 111
- 55 62 S. Behzadi, V. Serpooshan, W. Tao, M. A. Hamaly, M. Y. 112 85
- 56 Alkawareek, E. C. Dreaden, D. Brown, A. M. Alkilany, O. 113
- 57 Farokhzad and M. Mahmoudi, *Chem. Soc. Rev.*, 2017, **46**, 114 86
- 4218–4244.
- Y. Jiang, S. Huo, T. Mizuhara, R. Das, Y. W. Lee, S. Hou, D. F. Moyano, B. Duncan, X. J. Liang and V. M. Rotello, *ACS Nano*, 2015, **9**, 9986–9993.
- K. A. Dawson, A. Lesniak, F. Fenaroli, M. P. Monopoli, A. Christoffer and A. Salvati, *ACS Nano*, 2012, 5845–5857.
- J. Blechinger, A. T. Bauer, A. A. Torrano, C. Gorzelanny, C. Bräuchle and S. W. Schneider, *Small*, 2013, **9**, 3970–3980.
- S. Tatur, M. MacCarini, R. Barker, A. Nelson and G. Fragneto, *Langmuir*, 2013, **29**, 6606–6614.
- C. Montis, V. Generini, G. Boccalini, P. Bergese, D. Bani and D. Berti, *J. Colloid Interface Sci.*, 2018, **516**, 284–294.
- E. Fröhlich, *Int. J. Nanomedicine*, 2012, **7**, 5577–5591.
- J. A. Yang, S. E. Lohse and C. J. Murphy, *Small*, 2014, **10**, 1642–1651.
- E. Lee, H. Jeon, M. Lee, J. Ryu, C. Kang, S. Kim, J. Jung and Y. Kwon, *Sci. Rep.*, 2019, **9**, 2494.
- Y. C. Park, J. B. Smith, T. Pham, R. D. Whitaker, C. A. Sucato, J. A. Hamilton, E. Bartolak-Suki and J. Y. Wong, *Colloids Surfaces B Biointerfaces*, 2014, **119**, 106–114.
- J. Lin, H. Zhang, V. Morovati and R. Dargazany, *J. Colloid Interface Sci.*, 2017, **504**, 325–333.
- K. P. García, K. Zarschler, L. Barbaro, J. A. Barreto, W. O'Malley, L. Spiccia, H. Stephan and B. Graham, *Small*, 2014, **10**, 2516–2529.
- L. Zhang, H. Xue, C. Gao, L. Carr, J. Wang, B. Chu and S. Jiang, *Biomaterials*, 2010, **31**, 6582–6588.
- N. Gal, A. Lassenberger, L. Herrero-Nogareda, A. Scheberl, V. Charwat, C. Kasper and E. Reimhult, *ACS Biomater. Sci. Eng.*, 2017, **3**, 249–259.
- E. Giovanelli, E. Muro, G. Sitbon, M. Hanafi, T. Pons, B. Dubertret and N. Lequeux, *Langmuir*, 2012, **28**, 15177–15184.
- K. Kaaki, K. Hervé-Aubert, M. Chipier, A. Shkilnyy, M. Soucé, R. Benoit, A. Paillard, P. Dubois, M. L. Saboungi and I. Chourpa, *Langmuir*, 2012, **28**, 1496–1505.
- A. Kraus, L. Wortmann, L. Hermanns, N. Feliu, M. Vahter, S. Stucky, S. Mathur and B. Fadeel, *Nanomedicine Nanotechnology, Biol. Med.*, 2014, **10**, 1421–1431.
- X. Wang, X. Wang, X. Bai, L. Yan, T. Liu, M. Wang, Y. Song, G. Hu, Z. Gu, Q. Miao and C. Chen, *Nano Lett.*, 2019, **19**, 8–18.
- P. Vedantam, G. Huang and T. R. J. Tzeng, *Cancer Nanotechnol.*, 2013, **4**, 13–20.
- B. Pelaz, G. Charron, C. Pfeiffer, Y. Zhao, J. M. De La Fuente, X. J. Liang, W. J. Parak and P. Del Pino, *Small*, 2013, **9**, 1573–1584.
- M. P. Monopoli, D. Walczyk, A. Campbell, G. Elia, I. Lynch, F. Baldelli Bombelli and K. A. Dawson, *J. Am. Chem. Soc.*, 2011, **133**, 2525–2534.
- F. Bertoli, D. Garry, M. P. Monopoli, A. Salvati and K. A. Dawson, *ACS Nano*, 2016, **10**, 10471–10479.
- S. Milani, F. Baldelli Bombelli, A. S. Pitek, K. A. Dawson and J. Rädler, *ACS Nano*, 2012, **6**, 2532–2541.
- G. Caracciolo, O. C. Farokhzad and M. Mahmoudi, *Trends Biotechnol.*, 2017, **35**, 257–264.
- A. Lesniak, A. Salvati, M. J. Santos-Martinez, M. W.

- 1 Radomski, K. a. Dawson and C. Åberg, *J. Am. Chem. Soc.*, 58
- 2 2013, **135**, 1438–1444. 59
- 3 87 D. Hühn, K. Kantner, C. Geidel, S. Brandholt, I. De Cock, S. 60
- 4 H. Soenen, P. Riveragil, J. M. Montenegro, K. Braeckmans 61
- 5 K. Müllen, G. U. Nienhaus, M. Klapper and W. J. Parak, *ACS* 62
- 6 *Nano*, 2013, **7**, 3253–3263. 63
- 7 88 W. Lin, T. Insley, M. D. Tuttle, L. Zhu, D. A. Berthold, P. Kr 64
- 8 C. M. Rienstra and C. J. Murphy, *J. Phys. Chem. C*, 2015, 65
- 9 **119**, 21035–21043. 66
- 10 89 C. C. Fleischer and C. K. Payne, *Acc. Chem. Res.*, 2014, **47**, 67
- 11 2651–2659. 68
- 12 90 F. Wang, L. Yu, M. P. Monopoli, P. Sandin, E. Mahon, A. 69
- 13 Salvati and K. A. Dawson, *Nanomedicine Nanotechnology*, 70
- 14 *Biol. Med.*, 2013, **9**, 1159–1168. 71
- 15 91 L. Treuel, S. Brandholt, P. Maffre, S. Wiegele, L. Shang and 72
- 16 G. U. Nienhaus, *ACS Nano*, 2014, **8**, 503–513. 73
- 17 92 S. Fogli, C. Montis, S. Paccosi, A. Silvano, E. Michelucci, D. 74
- 18 Berti, A. Bosi, A. Parenti and P. Romagnoli, *Nanomedicine* 75
- 19 2017, **12**, 1647–1660. 76
- 20 93 R. P. Carney, T. M. Carney, M. Mueller and F. Stellacci, 77
- 21 *Biointerphases*, 2012, **7**, 17. 78
- 22 94 F. Simonelli, D. Bochicchio, R. Ferrando and G. Rossi, *J.* 79
- 23 *Phys. Chem. Lett.*, 2015, **6**, 3175–3179. 80
- 24 95 S. Li and N. Malmstadt, *Soft Matter*, 2013, **9**, 4969. 81
- 25 96 A. M. Farnoud and S. Nazemidashtarjandi, *Environ. Sci.* 82
- 26 *Nano*, 2019, **6**, 13–40. 83
- 27 97 A. Šarić and A. Cacciuto, *Soft Matter*, 2013, **9**, 6677–6695 84
- 28 98 K. Jaskiewicz, A. Larsen, D. Schaeffel, K. Koynov, I. 85
- 29 Lieberwirth, G. Fytas, K. Landfester and A. Kroeger, *ACS* 86
- 30 *Nano*, 2012, **6**, 7254–7262. 87
- 31 99 A. Šarić and A. Cacciuto, *Phys. Rev. Lett.*, 2012, **108**, 88
- 32 118101. 89
- 33 100 H. Zhang, Q. Ji, C. Huang, S. Zhang, B. Yuan, K. Yang and Y 90
- 34 Q. Ma, *Sci. Rep.*, 2015, **5**, 10525. 91
- 35 101 M. Raatz, R. Lipowsky and T. R. Weigl, *Soft Matter*, 2014, 92
- 36 **10**, 3570–3577. 93
- 37 102 A. H. Bahrami, R. Lipowsky and T. R. Weigl, *Phys. Rev. Lett.* 94
- 38 2012, **109**, 188102. 95
- 39 103 N. D. Burrows, A. M. Vartanian, N. S. Abadeer, E. M. 96
- 40 Grzincic, L. M. Jacob, W. Lin, J. Li, J. M. Dennison, J. G. 97
- 41 Hinman and C. J. Murphy, *J. Phys. Chem. Lett.*, 2016, **7**, 98
- 42 632–641. 99
- 43 104 S. Nangia and R. Sureshkumar, *Langmuir*, 2012, **28**, 17660 100
- 44 17671. 101
- 45 105 R. Vácha, F. J. Martinez-Veracochea and D. Frenkel, *Nano* 102
- 46 *Lett.*, 2011, **11**, 5391–5395. 103
- 47 106 Y. Qiu, Y. Liu, L. Wang, L. Xu, R. Bai, Y. Ji, X. Wu, Y. Zhao, 104
- 48 Li and C. Chen, *Biomaterials*, 2010, **31**, 7606–7619. 105
- 49 107 A. Espinosa, A. K. A. Silva, A. Sánchez-Iglesias, M. Grzelczak 106
- 50 C. Péchoux, K. Desboeufs, L. M. Liz-Marzán and C. Wilhelm 107
- 51 *Adv. Healthc. Mater.*, 2016, **5**, 1040–1048. 108
- 52 108 H. I. Ingólfsson, M. N. Melo, F. J. Van Eerden, C. Arnarez, 109
- 53 A. Lopez, T. A. Wassenaar, X. Periole, A. H. De Vries, D. P. 110
- 54 Tieleman and S. J. Marrink, *J. Am. Chem. Soc.*, 2014, **136**, 111
- 55 14554–14559. 112
- 56 109 T. Lunnoo, J. Assawakhajornsak and T. Puangmali, *J. Phys.* 113
- 57 *Chem. C*, 2019, **123**, 3801–3810. 114
- M. Laurencin, T. Georgelin, B. Malezieux, J. M. Siaugue and 115
- C. Ménager, *Langmuir*, 2010, **26**, 16025–16030. 116
- B. Wang, L. Zhang, S. C. Bae and S. Granick, *Proc. Natl.* 117
- Acad. Sci.*, 2008, **105**, 18171–18175. 118
- G. D. Bothun, N. Ganji, I. A. Khan, A. Xi and C. Bobba, 119
- Langmuir*, 2017, **33**, 353–360. 120
- T. Róg, M. Pasenkiewicz-Gierula, I. Vattulainen and M. 121
- Karttunen, *Biochim. Biophys. Acta - Biomembr.*, 2009, 122
- 1788, 97–121. 123
- E. S. Melby, A. C. Mensch, S. E. Lohse, D. Hu, G. Orr, C. J. 124
- Murphy, R. J. Hamers and J. A. Pedersen, *Environ. Sci.* 125
- Nano*, 2016, **3**, 45–55. 126
- D. Hartono, Hody, K. L. Yang and L. Y. Lanry Yung, 127
- Biomaterials*, 2010, **31**, 3008–3015. 128
- F. Lolicato, L. Joly, H. Martinez-Seara, G. Fragneto, E. 129
- Scoppola, F. Baldelli Bombelli, I. Vattulainen, J. Akola and 130
- M. Maccarini, *Small*, 2019, **15**, 1805046. 131
- R. Michel, E. Kesselman, T. Plostica, D. Danino and M. 132
- Gradzielski, *Angew. Chemie Int. Ed.*, 2014, **53**, n/a-n/a. 133
- S. Zhang, A. Nelson and P. A. Beales, *Langmuir*, 2012, **28**, 12831–12837.
- S. Chakraborty, A. Abbasi, G. D. Bothun, M. Nagao and C. L. 134
- Kitchens, *Langmuir*, 2018, **34**, 13416–13425. 135
- C. Montis, A. Zendrini, F. Valle, S. Busatto, L. Paolini, A. 136
- Radeghier, A. Salvatore, D. Berti and P. Bergese, *Colloids* 137
- Surfaces B Biointerfaces*, 2017, **158**, 331–338. 138
- C. Montis, D. Maiolo, I. Alessandri, P. Bergese and D. Berti, 139
- Nanoscale*, 2014, **6**, 6452–6457. 140
- J. C. Black, P. P. Cheney, T. Campbell and M. K. Knowles, 141
- Soft Matter*, 2014, **10**, 2016–2023. 142
- Y. Liu, R. Medda, Z. Liu, K. Galior, K. Yehl, J. P. Spatz, E. A. 143
- Cavalcanti-Adam and K. Salaita, *Nano Lett.*, 2014, **14**, 144
- 5539–5546. 145
- G. H. Zan, J. A. Jackman, S.-O. Kim and N.-J. Cho, *Small*, 146
- 2014, **10**, 4828–4832. 147
- O. Limaj, D. Etezadi, N. J. Wittenberg, D. Rodrigo, D. Yoo, S. 148
- H. Oh and H. Altug, *Nano Lett.*, 2016, **16**, 1502–1508. 149
- K. Suga, T. Yoshida, H. Ishii, Y. Okamoto, D. Nagao, M. 150
- Konno and H. Umakoshi, *Anal. Chem.*, 2015, **87**, 4772– 151
4780. 152
- D. Bhowmik, K. R. Mote, C. M. MacLaughlin, N. Biswas, B. 153
- Chandra, J. K. Basu, G. C. Walker, P. K. Madhu and S. Maiti, 154
- ACS Nano*, 2015, **9**, 9070–9077. 155
- K. Sugikawa, T. Kadota, K. Yasuhara and A. Ikeda, *Angew.* 156
- Chemie - Int. Ed.*, 2016, **55**, 4059–4063. 157
- C. Montis, S. Busatto, F. Valle, A. Zendrini, A. Salvatore, Y. 158
- Gerelli, D. Berti and P. Bergese, *Adv. Biosyst.*, 2018, **2**, 159
1700200. 160
- D. Maiolo, L. Paolini, G. Di Noto, A. Zendrini, D. Berti, P. 161
- Bergese and D. Ricotta, *Anal. Chem.*, 2015, **87**, 4168–4176. 162
- S. Busatto, A. Giacomini, C. Montis, R. Ronca and P. 163
- Bergese, *Anal. Chem.*, 2018, **90**, 7855–7861. 164
- A. Mallardi, N. Nuzziello, M. Liguori, C. Avolio and G. 165
- Palazzo, *Colloids Surfaces B Biointerfaces*, 2018, **168**, 134– 166
142. 167
- J. Zhai, C. Fong, N. Tran and C. J. Drummond, *ACS Nano*, 168
- 2019, **13**, acsnano.8b07961. 169

- 1 134 R. Mezzenga, J. M. Seddon, C. J. Drummond, B. J. Boyd, *G58*
- 2 E. Schröder-Turk and L. Sagalowicz, *Adv. Mater.*, 2019, **59** 156
- 3 **1900818**, 1–19. **60**
- 4 135 H. M. G. Barriga, M. N. Holme and M. M. Stevens, *Angew. 61*
- 5 *Chemie Int. Ed.*, 2019, **58**, 2958–2978. **62** 157
- 6 136 A. Salvatore, C. Montis, D. Berti and P. Baglioni, *ACS Nano*, **63**
- 7 2016, **10**, 7749–7760. **64** 158
- 8 137 O. Bixner and E. Reimhult, *J. Colloid Interface Sci.*, 2016, **65**
- 9 **466**, 62–71. **66** 159
- 10 138 R. Martínez-González, J. Estelrich and M. A. Busquets, *Int. 67*
- 11 *Mol. Sci.*, 2016, **17**, 1–14. **68**
- 12 139 B. Drasler, P. Budime Santhosh, D. Drobne, M. Erdani Krejcar, **69** 160
- 13 S. Kralj, D. Makovec and N. Poklar Ulrih, *Int. J.* **70**
- 14 *Nanomedicine*, 2015, **10**, 6089. **71** 161
- 15 140 S. Saesoo, S. Sathornsumetee, P. Anekwiang, C. **72**
- 16 Treetidnipa, P. Thuwajit, S. Bunthot, W. Maneeprakorn, **73** 162
- 17 Maurizi, H. Hofmann, R. U. Rungsardthong and N. **74**
- 18 Saengkrit, *Colloids Surfaces B Biointerfaces*, 2018, **161**, **75** 163
- 19 497–507. **76**
- 20 141 E. Amstad, J. Kohlbrecher, E. Müller, T. Schweizer, M. **77** 164
- 21 Textor and E. Reimhult, *Nano Lett.*, 2011, **11**, 1664–1670. **78** 165
- 22 142 S. Nappini, S. Fogli, B. Castroflorio, M. Bonini, F. Baldelli **79**
- 23 Bombelli and P. Baglioni, *J. Mater. Chem. B*, 2016, **4**, 716–**80** 166
- 24 725. **81**
- 25 143 J. Haša, J. Hanuš and F. Štěpánek, *ACS Appl. Mater. **82*** 167
- 26 *Interfaces*, 2018, **10**, 20306–20314. **83**
- 27 144 P. Pradhan, J. Giri, F. Rieken, C. Koch, O. Mykhaylyk, M. **84** 168
- 28 Döblinger, R. Banerjee, D. Bahadur and C. Plank, *J. Control. **85***
- 29 *Release*, 2010, **142**, 108–121. **86** 169
- 30 145 R. Di Corato, G. Béalle, J. Kolosnjaj-Tabi, A. Espinosa, O. **87**
- 31 Clément, A. K. A. Silva, C. Ménager and C. Wilhelm, *ACS **88*** 170
- 32 *Nano*, 2015, **9**, 2904–2916. **89**
- 33 146 A. K. Rengan, A. B. Bukhari, A. Pradhan, R. Malhotra, R. **90** 171
- 34 Banerjee, R. Srivastava and A. De, *Nano Lett.*, 2015, **15**, **91**
- 35 842–848. **92** 172
- 36 147 A. Tomitaka, H. Arami, Z. Huang, A. Raymond, E. Rodriguez, **93**
- 37 Y. Cai, M. Febo, Y. Takemura and M. Nair, *Nanoscale*, 2018, **10**, 184–194. **94** 173
- 38 **10**, 184–194. **95**
- 39 148 M. E. Khosroshahi, *J. Nanomed. Nanotechnol.*, **96** 174
- 40 DOI:10.4172/2157-7439.1000298. **97**
- 41 149 R. B. Lira, M. A. B. L. Seabra, A. L. L. Matos, J. V. **98**
- 42 Vasconcelos, D. P. Bezerra, E. De Paula, B. S. Santos and A. **99** 175
- 43 Fontes, *J. Mater. Chem. B*, 2013, **1**, 4297–4305. **100**
- 44 150 M. Wlodek, M. Kolasinska-Sojka, M. Szuwarzynski, S. **101** 176
- 45 Kereiche, L. Kovacic, L. Zhou, L. Islas, P. Warszynski and **102**
- 46 H. Briscoe, *Nanoscale*, 2018, **10**, 17965–17974. **103**
- 47 151 J. B. Marlow, M. J. Pottage, T. M. McCoy, L. De Campo, **104** 177
- 48 Sokolova, T. D. M. Bell and R. F. Tabor, *Phys. Chem. Chem. **105***
- 49 *Phys.*, 2018, **20**, 16592–16603. **106**
- 50 152 J. J. Vallooran, R. Negrini and R. Mezzenga, *Langmuir*, 2011, **29**, 999–1004. **107** 178
- 51 **29**, 999–1004. **108**
- 52 153 J. J. Vallooran, S. Handschin, S. Bolisetty and R. Mezzenga, **109**
- 53 *Langmuir*, 2012, **28**, 5589–5595. **110** 179
- 54 154 J. J. Vallooran, S. Bolisetty and R. Mezzenga, *Adv. Mater.* **111**
- 55 2011, **23**, 3932–3937. **112** 180
- 56 155 W. K. Fong, T. L. Hanley, B. Thierry, A. Tilley, N. Kirby, L. **113**
- 57 Waddington and B. J. Boyd, *Phys. Chem. Chem. Phys.*, 2011, **14**, **114**
- 16, 24936–24953.
- W. K. Fong, T. L. Hanley, B. Thierry, N. Kirby, L. J. Waddington and B. J. Boyd, *Langmuir*, 2012, **28**, 14450–14460.
- S. M. Moghimi, A. C. Hunter and T. L. Andresen, *Annu. Rev. Pharmacol. Toxicol.*, 2011, **52**, 481–503.
- S. Mitragotri and J. Lahann, *Adv. Mater.*, 2012, **24**, 3717–3723.
- W. H. De Jong, W. I. Hagens, P. Krystek, M. C. Burger, A. J. A. M. Sips and R. E. Geertsma, *Biomaterials*, 2008, **29**, 1912–1919.
- P. Aggarwal, J. B. Hall, C. B. McLeland, M. A. Dobrovolskaia and S. E. McNeil, *Adv. Drug Deliv. Rev.*, 2009, **61**, 428–437.
- T. A. Wynn, A. Chawla and J. W. Pollard, *Nature*, 2013, **496**, 445–55.
- B. Illes, P. Hirschle, S. Barnert, V. Cauda, S. Wuttke and H. Engelke, *Chem. Mater.*, 2017, **29**, 8042–8046.
- K. Raemdonck, K. Braeckmans, J. Demeester and S. C. De Smedt, *Chem. Soc. Rev.*, 2014, **43**, 444–472.
- A. Luchini and G. Vitiello, *Front. Chem.*, 2019, **7**, 1–16.
- M. E. Davis, Z. Chen and D. M. Shin, *Nat. Rev. Drug Discov.*, 2008, **7**, 771–782.
- N. Kamaly, Z. Xiao, P. M. Valencia, A. F. Radovic-Moreno and O. C. Farokhzad, *Chem. Soc. Rev.*, 2012, **41**, 2971.
- Z. Shen, H. Ye, M. Kröger and Y. Li, *Phys. Chem. Chem. Phys.*, 2017, **19**, 13294–13306.
- A. Luchini, R. K. Heenan, L. Paduano and G. Vitiello, *Phys. Chem. Chem. Phys.*, 2016, **18**, 18441–18449.
- T. M. Allen and P. R. Cullis, *Adv. Drug Deliv. Rev.*, 2013, **65**, 36–48.
- E. Terreno, F. Uggeri and S. Aime, *J. Control. Release*, 2012, **161**, 328–337.
- R. Rapuano and A. M. Carmona-Ribeiro, *J. Colloid Interface Sci.*, 1997, **193**, 104–111.
- R. Rapuano and A. M. Carmona-Ribeiro, *J. Colloid Interface Sci.*, 2000, **226**, 299–307.
- A. L. Troutier and C. Ladavière, *Adv. Colloid Interface Sci.*, 2007, **133**, 1–21.
- F. Mousseau, C. Puisney, S. Mornet, R. Le Borgne, A. Vacher, M. Airiau, A. Baeza-Squiban and J. F. Berret, *Nanoscale*, 2017, **9**, 14967–14978.
- L. M. Rossi, P. R. Silva, L. L. R. Vono, A. U. Fernandes, D. B. Tada and M. S. Baptista, *Langmuir*, 2008, **24**, 12534–12538.
- D. B. Tada, E. Suraniti, L. M. Rossi, C. A. P. Leite, C. S. Oliveira, T. C. Tumolo, R. Calemczuk, T. Livache and M. S. Baptista, *J. Biomed. Nanotechnol.*, 2014, **10**, 519–528.
- S. A. Mackowiak, A. Schmidt, V. Weiss, C. Argyo, C. Von Schirnding, T. Bein and C. Bräuchle, *Nano Lett.*, 2013, **13**, 2576–2583.
- Q. Zhang, X. Chen, H. Shi, G. Dong, M. Zhou, T. Wang and H. Xin, *Colloids Surfaces B Biointerfaces*, 2017, **160**, 527–534.
- S. Chernousova and M. Eppe, *Angew. Chemie - Int. Ed.*, 2013, **52**, 1636–1653.
- R. R. Arvizo, S. Bhattacharyya, R. A. Kudgus, K. Giri, R. Bhattacharya and P. Mukherjee, *Chem. Soc. Rev.*, 2012, **41**, 2943.

- 1 181 L. Cheng, M. D. Weir, H. H. K. Xu, J. M. Antonucci, N. J. Lin,
2 S. Lin-Gibson, S. M. Xu and X. Zhou, *J. Biomed. Mater. Res.*
3 *Part B Appl. Biomater.*, 2012, **100B**, 1378–1386.
- 4 182 B. Du, L. Tian, X. Gu, D. Li, E. Wang and J. Wang, *Small*,
5 2015, **11**, 2333–2340.
- 6 183 C. G. England, A. M. Gobin and H. B. Frieboes, *Eur. Phys. J.*
7 *Plus*, 2015, **130**, 231.
- 8 184 H. Frieboes, C. England, T. Priest, G. Zhang, X. Sun, D. Patel,
9 L. McNally, V. van Berkel and A. Gobin, *Int. J.*
10 *Nanomedicine*, 2013, 3603.
- 11 185 D. J. Hamilton, M. D. Coffman, J. D. Knight and S. M. Reed,
12 *Langmuir*, 2017, **33**, 9222–9230.
- 13 186 P. Wang, L. Zhang, W. Zheng, L. Cong, Z. Guo, Y. Xie, L.
14 Wang, R. Tang, Q. Feng, Y. Hamada, K. Gonda, Z. Hu, X. Wu
15 and X. Jiang, *Angew. Chemie - Int. Ed.*, 2018, **57**, 1491–
16 1496.
- 17 187 R. Liang, J. Xie, J. Li, K. Wang, L. Liu, Y. Gao, M. Hussain, G.
18 Shen, J. Zhu and J. Tao, *Biomaterials*, 2017, **149**, 41–50.
- 19 188 B. K. Poudel, B. Gupta, T. Ramasamy, R. K. Thapa, S. Pathak,
20 K. T. Oh, J. H. Jeong, H. G. Choi, C. S. Yong and J. O. Kim,
21 *Colloids Surfaces B Biointerfaces*, 2017, **160**, 73–83.
- 22 189 C. J. Orendorff, T. M. Alam, D. Y. Sasaki, B. C. Bunker and J.
23 A. Voigt, *ACS Nano*, 2009, **3**, 971–983.
- 24 190 P. B. Santhosh, N. Thomas, S. Sudhakar, A. Chadha and E.
25 Mani, *Phys. Chem. Chem. Phys.*, 2017, **19**, 18494–18504.
- 26 191 E. T. Castellana, R. C. Gamez and D. H. Russell, *J. Am. Chem.*
27 *Soc.*, 2011, **133**, 4182–4185.
- 28 192 X. Cui, W. Cheng and X. Han, *J. Mater. Chem. B*, 2018, **6**,
29 8078–8084.
- 30 193 Y. Ma, S. Tong, G. Bao, C. Gao and Z. Dai, *Biomaterials*,
31 2013, **34**, 7706–7714.
- 32 194 A. Ruiz-De-Angulo, A. Zabaleta, V. Gómez-Vallejo, J. Llop
33 and J. C. Mareque-Rivas, *ACS Nano*, 2016, **10**, 1602–1618.
- 34 195 G. Traini, A. Ruiz-de-Angulo, J. B. Blanco-Canosa, K.
35 Zamacola Bascarán, A. Molinaro, A. Silipo, D. Escors and J.
36 C. Mareque-Rivas, *Small*, DOI:10.1002/sml.201803993.
- 37 196 J. Liang, X. Zhang, Y. Miao, J. Li and Y. Gan, *Int. J.*
38 *Nanomedicine*, 2017, **12**, 2033–2044.
- 39 197 A. Torchi, F. Simonelli, R. Ferrando and G. Rossi, *ACS Nano*,
40 2017, **11**, 12553–12561.
- 41